공학박사학위논문

WiFi 및 UWB 통신 시스템을 위한 자원 관리 방법에 관한 연구

Study on Resource Management Methods
for WiFi and UWB Communication Systems

2021년 2월

서울대학교 대학원

전기·컴퓨터공학부

오 현 섭

WiFi 및 UWB 통신 시스템을 위한 자원 관리 방법에 관한 연구

Study on Resource Management Methods
for WiFi and UWB Communication Systems
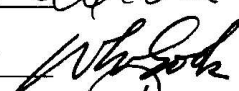
지도 교수 전 화 숙

이 논문을 공학박사 학위논문으로 제출함
2020년 12월

서울대학교 대학원
전기·컴퓨터 공학부
오 현 섭

오현섭의 박사 학위논문을 인준함
2020년 12월

위 원 장	김 종 권		
부위원장	전 화 숙		
위 원	권 태 경		
위 원	정 동 근		
위 원	박 세 웅		

Abstract

Study on Resource Management Methods for WiFi and UWB Communication Systems

Hyun Seob Oh

The School of Electrical Engineering and Computer Science

The Graduate School

Seoul National University

Nowadays, to support various services (e.g., multimedia content delivery, high definition video streaming, file download) on mobile devices, IEEE 802.11-based wireless local area network (WLAN) technologies have been widely used. Also, IEEE 802.15.4z based ultra-wideband (UWB) based ranging technique which can provide highly precise indoor localization services (e.g., human/object tracking systems in factory/office environment, location-based smart home applications) has attracted attention of global mobile device vendors. In this thesis, we study resource management methods that efficiently support WiFi and UWB devices while satisfying requirements of those devices, such as throughput and energy efficiency. First, we design a radio resource management (RRM) method in the dense WLAN environment. The proposed RRM method is composed of two phases: channel assignment (CA), user association for channel load balancing (UA-ChLB). In the CA phase, a centralized controller assigns channel and bandwidth of each AP where two types of APs coexist: controlled-APs (C-APs), which are managed by a centralized controller, and stand-alone APs (S-APs), which independently operate for

themselves. In this phase, channel usages of neighboring S-APs and interference level of C-APs according to the channel bonding are jointly considered to minimize interference among the APs. In the UA-ChLB phase, the user association between stations (STAs) and APs having low channel load is coordinated to maximize the overall network resource efficiency under consideration of time varying wireless channel and traffic conditions. To do this, the centralized controller periodically carries out the centralized UA-ChLB work with longer period, and each STA can change its serving AP and/or the serving channel at any time through the distributed UA-ChLB work. Second, we design a time resource management (TRM) method for IEEE 802.15.4z based UWB ranging systems which support highly precise spatial awareness and indoor localization services. Considering requirements for a ranging interval that may be different according to each application or device type, we design the ranging interval decision scheme based on Markov decision process to enhance the energy efficiency and satisfaction degree of UWB ranging devices (RDEVs). By simulation and experimental results, it is shown that the proposed RRM method for dense WLAN environment achieves its design goal and outperforms existing schemes from view point of throughput and fairness. Also, according to simulation, it is depicted that the proposed TRM for UWB ranging systems outperforms existing schemes for the energy efficiency and satisfaction level of RDEVs.

Keywords: IEEE 802.11 based WLAN, radio resource management, channel assignment, user association, IEEE 802.15.4z based UWB ranging system, time resource management, ranging interval

Student Number: 2012-23223

Contents

iv

List of Figures

List of Tables

Chapter 1. Introduction

1.1 Background and Motivation

Since IEEE 802.11-based wireless local area network (WLAN) technologies effectively support various services (e.g., multimedia contents delivery, full HD video streaming, file download), WLAN technologies have been widely used. Also, for supporting highly precise indoor localization services such as human/object tracking in factory/office environments, ultra-wideband (UWB) ranging technique has recently attracted a great attention. To satisfy requirements (e.g., throughput, energy saving) of WiFi and UWB devices and to enhance the efficiency of WiFi and UWB communication systems, elaborate resource management methods are essential. In the thesis, we focus on radio resource management (RRM) in the dense WLAN environment and time resource management (TRM) in the UWB ranging system.

According to extensive experiments conducted at a huge underground shopping mall [1], in the dense WLAN environment where APs are densely deployed (e.g., public, residential, and enterprise areas), the network performance may be severely degraded due to capacity reduction by channel sharing and interference among neighboring APs. This is because the service coverage of neighboring APs can overlap each other and the neighboring APs can commonly use the same channels. To effectively overcome the network performance degradation under such environment, it is essential to elaborately manage radio resource. The representative RRM techniques are channel assignment (CA) to reduce interference among neighboring APs and user association for balancing network load among APs (UA-LB). Since IEEE 802.11 standard such as IEEE 802.11n/ac allows the channel

bonding to support high potential capacity, researchers should design RRM methods while considering the characteristics of dense WLAN environment such as not only channel sharing and interference but also channel bonding.

There are various CA schemes to minimize the interference among APs [2–8]. However, there are few works which take account of channel bonding and interference together under the dense WLAN environment. Moreover, according to previous work in [9], coarsely utilization of channel bonding in CA may rather degrade the network performance by causing limited channel sharing and excessive interference. For this reason, an elaborate CA scheme which effectually avoids interference under channel bonding is necessary. The existing CA schemes in [3–9] can be categorized into centralized CA [6–9] and distributed CA [3–5], depending on whether there is a central coordinator allocating channels to all APs, or not. In distributed CA, each AP determines its operating channel for itself, without any controller. In the automatic channel selection (ACS) scheme [3], each AP selects a basic channel having the lowest interference after scanning available channels. With the random channel selection (RCS) scheme in [4], an AP selects consecutive basic channels for bonding at random from available channels. In the CA scheme of [5], an AP selects the channel with the lowest potential interference as its operating channel, where the potential interference from neighbor APs can be calculated based on traffic state information within the beacon frame. In the centralized CA schemes [6–8], a centralized controller decides the channel allocation for C-APs, by using various information reported from these C-APs. In [6], the CA problem is formulated as a maximum weight matching problem on bipartite graph and is solved by the Hungarian method, where the weight of each channel is calculated based on the estimated interference level of the channel. In the CA scheme of [7],

2

the controller collects the interference level among C-APs, and allocates the basic channels to C-APs so that the total interference level among APs through the entire network is minimized. A graph coloring-based CA scheme in [8] determines an appropriate primary channel of each AP, when a bonding channel is already given to each AP.

When designing a UA-LB scheme, band characteristic should be considered, since the property of radio propagation and configuration of overlapped channels are different depending on whether the frequency band of channel is 2.4 GHz or 5 GHz. Typically, co-channel interference (CCI) and adjacent channel interference (ACI) among neighboring APs are much more serious in 2.4 GHz than in 5 GHz band. Therefore, the interference coordination is much more important in 2.4 GHz band channels. Although most of commercial APs concurrently support dual-band of 2.4 GHz and 5 GHz, the previous studies of designing the UA-LB in [10–17] did not take account of the above mentioned band characteristics. Only few works related to band-steering (BSTR) (e.g., [18] and [19]) intend to balance the load between two frequency bands of one AP, through UA.

The UA schemes in [10–17] can also be categorized into distributed UA [10–13] and centralized UA [14–17]. In the distributed UA where each STA selects its AP for itself, the metric for AP selection is different in each scheme. Under the FAME scheme [10], a STA selects the best AP for maximizing the MAC efficiency metric, which is derived based on the link rate, traffic amount, and collision rate. In [11], a STA is associated with an AP having the highest SINR (signal to interference plus noise ratio). With the Wi-Fi seeker scheme in [12], each STA chooses an AP having the lowest interference level which can be estimated by measuring the beacon collision rate and RSSI (received signal strength indicator) variation. In [13], a

STA calculates the expected throughput from each AP by using the broadcasted channel occupancy information from neighboring APs and STAs, and selects the AP with the highest expected throughput. The centralized UA schemes have a central coordinator which determines UA for all STAs over the entire network. In [14], the authors take account of the effect due to interference among APs sharing the same channel and formulate a proportional fair UA problem. This UA problem is relaxed into a convex optimization problem and its solution is got by solving the relaxed problem. In [15], the authors define a fittingness factor, which indicates the UA suitability and is calculated by the utility function based on the SINR and quality-of-service (QoS) requirement of each STA. Then, the UA between each STA and AP aims at maximizing the fittingness factor. The UA scheme in [16] distributes the load among APs to maximize the overall network throughput. To solve this UA problem in the dense WLAN environment, authors in [16] transform it into a weighted bipartite graph matching problem and solve it by finding the semi-optimal matching of the graph. The UA scheme in [17] puts some APs with low load into a sleep mode. Then, the STAs associated with these sleeping APs are moved into other APs so that the load among active APs is well balanced. Also, BSTR-based UA schemes in [18] and [19] intend to balance the load between the 2.4 GHz-channel and the 5 GHz-channel within one AP. In [18], the STAs within one AP are distributed into two frequency bands, based on the number of STAs in each band and channel quality. This BSTR scheme tries to maintain a predefined ratio between the number of associated users in 2.4 GHz band and that in 5 GHz band. When recognizing the congestion in 2.4 GHz band, the STA currently associated with 2.4 GHz-channel can adjust its own UA to a 5 GHz-channel, if SNR and RSSI in the 5 GHz-channel are higher than the predefined SNR and RSSI thresholds.

4

In [19], the BSTR between two frequency bands are determined based on RSSI, medium occupancy ratio, and past BSTR results. When the medium occupancy ratio of 2.4 GHz band is relatively high, some STAs in 2.4 GHz band can be moved into 5 GHz band while satisfying the RSSI requirement in 5 GHz.

On the other hand, the usefulness of UWB for ranging is in the limelight. Since the UWB utilizes a wide bandwidth over 500 MHz between 3.1 and 10.6 GHz band, its frequency characteristics (e.g., robustness against interference, propagation straightness) have the inherent benefit for highly precise ranging. Therefore, time-of-flight (ToF) can be calculated with a high time-resolution. The ToF-based ranging with the high time-resolution can effectively support a highly precise spatial awareness and indoor localization. The UWB ranging technique is being standardized as the IEEE 802.15.4z [41] and this standard aims to adopt new capabilities using UWB into the PHY/MAC layers of the existing IEEE 802.15.4a, IEEE 802.15.4f, and IEEE 802.15.4-–2015 standards [42] – [44]. The PHY layer enhancements in IEEE 802.15.4z, such as a scrambled timestamp sequence to measure the ToF, supports a highly secured ranging which prevents accidental interference or malicious capture of timestamp sequence [45], [46]. Furthermore, the MAC layer enhancements in IEEE 802.15.4z enable a highly accurate ranging and efficiently support various ranging scenarios composed of multiple devices [46]. For these reasons, it is expected that IEEE 802.15.4z based UWB ranging will be widely used in various applications that exploit the highly precise and secured localization information. The representative use cases include the human/object tracking systems in factory/office environment, the proximity-based services such as adaptive cruise control for vehicles and car door lock, and the location-based smart home applications such as light control, door lock, and air conditioning systems.

5

For this reason, several chipset vendors (e.g., Samsung, NXP, and Qorvo) participating in the standardization of IEEE 802.15.4z have organized the Fira (which stands for "fine ranging") consortium to develop UWB ranging use cases and to promote UWB ecosystems [46]. Also, Apple which is one of leading vendors of mobile devices recently has released mobile devices supporting the UWB-based ranging through U1 chipset, and other global leading vendors such as Samsung, Xiaomi, recently introduce the UWB ranging function into their new mobile devices.

According to the IEEE 802.15.4z standard, multiple ranging devices (RDEVs) can compose a ranging group. In each group, there is a single controller supervising the ranging operation of the group. The UWB ranging for each group is performed once every ranging block. Thus, the length of a ranging block corresponds to the time interval of ranging operations. The controller determines the length of a ranging block and schedules the time resource so that the RDEVs can exchange messages for ranging. When a ranging group is composed of devices with various and different applications, requirements for a ranging block length may be different according to each application or device type. For example, devices that should survive for a long time with a small battery may prefer a long block length to reduce the energy consumption, whereas mission critical applications may require a very short block length to quickly acquire the ranging result. Furthermore, since the state of a device such as moving speed or battery level usually varies with time, the required block length of a device may change for each ranging block.

1.2 Proposed Resource Management Methods for WiFi and UWB Communication Systems

1.2.1 Radio Resource Management (RRM) for Dense WLAN Environment

In the dense WLAN environment of real world, there coexist two types of APs: controlled-APs (C-APs), managed by a centralized controller, and stand-alone APs (S-APs), each of which independently operates. S-APs and C-APs may suffer from severe interference (i.e., CCI and/or ACI) from each other, if their radio resource utilization is not carefully managed. Thus, this coexistence can greatly affect the CA results for C-APs and the UA-LB decision. However, the coordination between S-APs and C-APs is a difficult problem because recognizing the status information (e.g., load, amount of traffic, interference level) of the other type of APs is not easy. To our best knowledge, except for few CA schemes such as [6] and [9], there is no published study of the RRM including both CA and UA-LB, under the dense WLAN environment where C-APs and S-APs coexist.

In the thesis, we suggest two-phase RRM method composed of CA and UA-LB, in the dense WLAN environment where two types of APs coexist and each of WLAN devices (i.e., S-APs, C-APs, and STAs) supports dual-band of 2.4 GHz and 5 GHz by using two wireless network interfaces. The proposed RRM method comprehensively takes current overall network conditions (e.g., wireless channel quality, interference, the amount of traffic) into account.

1.2.2 Time Resource Management (TRM) for UWB Ranging Systems

In the UWB ranging system complying with IEEE 802.15.4z [41], a controller needs to determine a block length of its ranging group, taking account of the requirements or state changes of the RDEVs. This is because the block length decision has a great effect on the energy consumption or ranging interval of the RDEVs. However, to our best knowledge, there is no published study of the block length decision for IEEE 802.15.4z, because the standardization of IEEE 802.15.4z has been very recently completed.

In the thesis, we design a novel decision scheme to efficiently determine the block length of a ranging group, under consideration of the ranging requirements of RDEVs in the ranging group. We model the overall process for determining the block length as a Markov decision process (MDP), where the system reward is designed based on the energy consumption and the satisfaction level of RDEVs. Through the proposed MDP-based TRM, the controller can determine a ranging block length to maximize the system reward.

1.3 Organization

The remainder of the thesis is organized as follows. Chapter 2 describes the RRM method for the dense WLAN environment where dual bands are supported and two types of APs coexist. In Section 2.1, the system model under consideration is explained. We suggest a two-phase RRM framework in dense WLAN environment in Section 2.2. Section 2.3 describes the proposed UA-LB scheme.

Chapter 3 describes a novel MDP-based decision scheme of the ranging block length. We briefly explain the IEEE 802.15.4z ranging operation focusing on the ranging block length in Section 3.1, and describes the proposed scheme based on MDP in Section 3.2.

In Chapter 4, we present the performance evaluation of two resource management methods. In Section 4.1, we show the performance of the proposed RRM method. We implement the proposed RRM method and some existing schemes, and assess their performances based on the experimental results. Also, we present their performances on the simulation results. In Section 4.2, we present the simulation results of the proposed MDP-based block length method and compared schemes. Finally, the thesis is concluded with Chapter 5.

Chapter 2.   Radio Resource Management in Dense WLAN Environment

2.1   System Model

In this section, we describe the system model under consideration and input parameters of RRM scheme. Fig. 2.1 depicts the system model under consideration, representing dense WLAN environment. There coexist two types of APs: C-APs and S-APs. The C-APs are connected to a centralized controller through wired link (e.g., Ethernet) and thus the controller can acquire directly from each C-AP various information, such as the number of associated STAs, traffic arrival rates of STAs, and transmission rate. Each S-AP operates independently, so that the controller cannot directly obtain information from S-APs. All of C-APs and S-APs are dual-band APs supporting both 2.4 GHz and 5 GHz bands.

The STAs are classified into legacy STA (L-STA) and non-legacy STA (NL-STA). The L-STA is a typical IEEE 802.11 STA where the association of STA with AP is determined based on the RSSI, whereas the NL-STA is an IEEE 802.11 STA where the proposed scheme is additionally implemented. The NL-STAs are again subdivided into two types, according to whether the NL-STA is associated with C-AP or S-AP. The NL-STA associated with C-AP is referred to as C-STA, and the NL-STA associated with S-AP is referred to as S-STA.

2.1.1   Input Parameters of Two-Phase RRM

We will suggest, in the next section, a two-phase RRM framework for enhancing WLAN performance under the above system model, which is composed of the CA in the first phase and the UA-LB in the second phase (see Fig. 2.2).
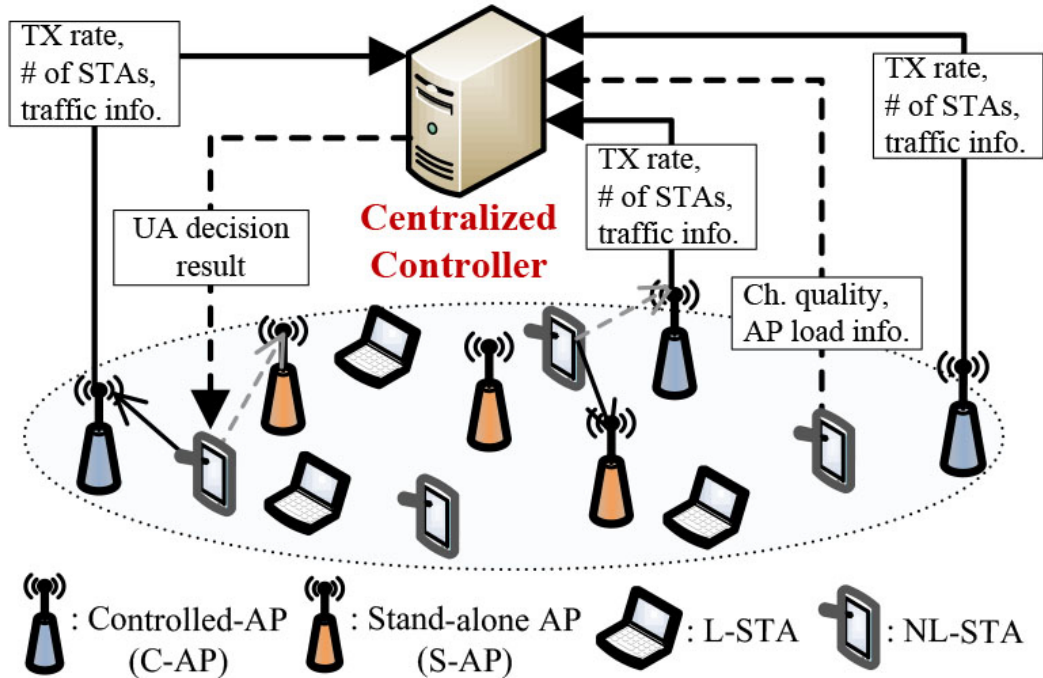
Fig. 2.1: System model
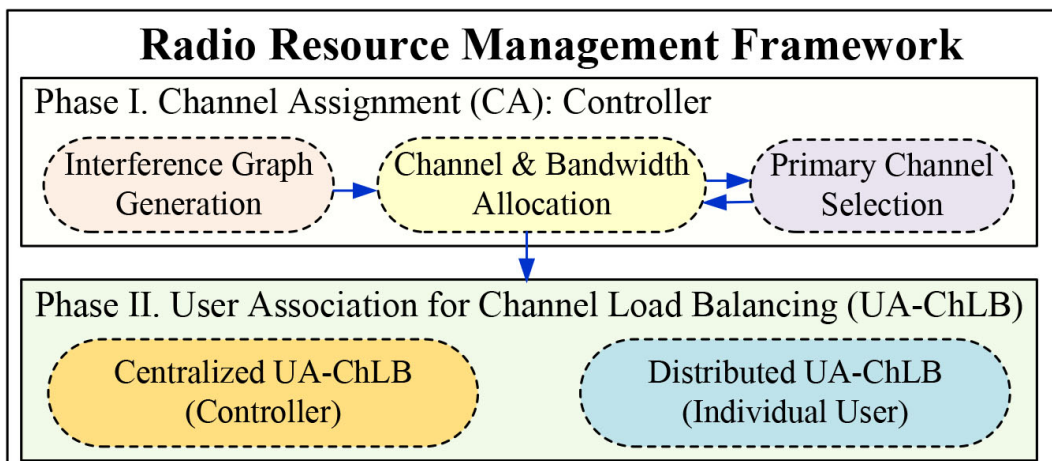
Fig. 2.2: Proposed RRM Framework

Since interference signal causes the performance degradation, it is desirable to allocate different channels if possible, for APs being potential interferer to each other. Thus, the prerequisite task of CA is to identify, for each AP, its interfering APs. On the other hand, since the goal of our UA-LB work is to improve channel efficiency by appropriately balancing the load in the viewpoint of entire network, we need to firstly estimate the load and channel efficiency prior to specifically designing the UA-LB scheme. Now, we examine input parameters for two-phase RRM exemplified above, in more detail.

Interfering AP

As mentioned above, in allocating channels to APs, it is essential to investigate interference relationship among APs. As the criteria of detecting such interference relationship, we use the minimum clear channel assessment (CCA) threshold of IEEE 802.11. Let $\xi_{\text{CCA-CS}}$ be the minimum threshold for carrier sense-based CCA of a basic channel. Note that $\xi_{\text{CCA-CS}} = -82$ dBm for a single basic channel (20 MHz) in IEEE 802.11. Let us consider the situation that, while AP-l is transmitting on a channel, another AP-k does carrier sensing on the same channel. If the AP-k detects the signal strength stronger than $\xi_{\text{CCA-CS}}$, the AP-k regards the channel as being busy and does not access the channel. Then, the AP-l is referred to as a directly interfering AP of AP-k.

On the other hand, some channels on ISM band are overlapped with each other. Unlike 5 GHz band where most of channels are not overlapped, adjacent channels in 2.4 GHz band are overlapped each other except three channels known as channel 1, 6, 11. Although two neighboring APs use different channels, if their channels are overlapped, these APs can suffer from severe adjacent-channel-interference (ACI)

Tab. 2.1: Power leakage ratio (2.4 GHz)

Channel distance	1	2	3	4	5
Leakage ratio (%)	79.06	52.67	26.51	0.627	0.121

from each other. We calculate the ACI at AP-k from neighboring AP-l, based on the RSSI at AP-k from AP-l and the ratio of leakage power (i.e., power leakage ratio) from the channel of AP-l to the channel of AP-k. According to [23] and [24], the power leakage ratio of two channels depends on the distance between them, i.e., the lower ratio from a channel being farther away. We define the number difference of two channels as the channel distance between them. Let $d(k, l)$ be the channel distance between the channels of AP-k and AP-l. And, let $\rho_{d(k,l)}$ denote the power leakage ratio for the channel distance of $d(k, l)$. Table 2.1 shows the power leakage ratio with respect to channel distance in 2.4 GHz band of 802.11 WLAN, referred from [23] and [24]. When $RSSI(k, l)$ is the RSSI value for beacon of AP-l measured by AP-k, the ACI at AP-k from AP-l, denoted by $\mathcal{I}_{ACI}(k, l)$, is calculated as follows.

$$\mathcal{I}_{ACI}(k, l) = \rho_{d(k,l)} \times RSSI(k, l). \tag{2.1}$$

If the ACL between two adjacent APs using different channels is higher than a predefined threshold, they can be the interfering AP to each other. We define another CCA threshold based on energy detection, $\xi_{\text{CCA-ED}}$. When $\mathcal{I}_{ACI}(k, l) > \xi_{\text{CCA-ED}}$, the AP-$l$ is also referred to as a directly interfering AP of AP-k although these two APs do not use the same channel. Note that $\xi_{\text{CCA-ED}} = -62$ dBm for a single basic channel of 20 MHz in IEEE 802.11.

On the other hand, consider that AP-k is outside the carrier sensing coverage of

AP-l but some STAs of AP-k is within the carrier sensing coverage of AP-l. Note that this is a very common situation where the coverage areas of two APs are partly overlapped. Then, since AP-k cannot detect transmission of AP-l, AP-l is not a directly interfering AP of AP-k. However, the STAs of AP-k within overlapped area can detect transmission of AP-l and their transmission can be disturbed by AP-l. We define that the AP-l and AP-k have a hidden interference relationship between them and are a hidden interferer of each other. The interference relationship among APs is used as input of the CA process.

Broadcast Information of AP

Each AP, irrespective of its type (i.e., C-AP or S-AP), broadcasts the following status information for each of two bands, through beacon frames: the number of associated STAs, the channel load, and average spectral efficiency. This information is used to realize the proposed scheme and is calculated as follows.

Let $\mathcal{S}(k, B)$ denote the set of STAs associated with the band-B channel of AP-k, where B is 2.4 GHz or 5 GHz. When $|s|$ denotes the cardinality of a set s, $|\mathcal{S}(k, B)|$ is the number of associated STAs for the band-B channel of AP-k. Let us define the channel load as the channel occupancy time portion for transmitting the traffic of all associated STAs. For the STA-i associated with AP-k in band-B, when α_i is the traffic arrival rate of STA-i and $C_{k,i}$ is the link rate between AP-k and STA-i, the channel time portion for transmitting the traffic of STA-i is calculated as $\frac{\alpha_i}{C_{k,i}}$. Then, we calculate the channel load of AP-k in band-B, denoted by $L(k, B)$, like in [17].

$$L(k, B) = \sum_{i \in \mathcal{S}(k,B)} \frac{\alpha_i}{C_{k,i}}, \tag{2.2}$$

14

Next, we calculate the average spectral efficiency (SE) for the band-B channel of AP-k, denoted by $\Gamma(k,B)$. Let $SNR_{k,i}$ be the signal-to-noise ratio (SNR) between AP-k and STA-i. According to [20], for given $SNR_{k,i}$, the average SE between AP-k and STA-i is

$$f\left(SNR_{k,i}\right) = \min\left(2.7, \ \log_2\left(1 + 0.25 \cdot SNR_{k,i}\right)\right). \tag{2.3}$$

Then, according to [21] and [22], $\Gamma(k,B)$ is calculated as the harmonic mean of the SEs of associated STAs.

$$\Gamma(k,B) = \frac{|\mathcal{S}(k,B)|}{\sum_{i \in \mathcal{S}(k,B)} \frac{1}{f\left(SNR_{k,i}\right)}}. \tag{2.4}$$

The AP-k broadcasts $|\mathcal{S}(k,B)|$, $L(k,B)$, and $\Gamma(k,B)$ for each band-B channel, through beacon frame. These are used for UA-LB work.

2.2 Two-Phase RRM Framework in dense WLAN environment

In this section, we suggest a two-phase RRM framework for enhancing network performance in a typical dense WLAN environment of Fig. 1. The suggested two-phase RRM framework is depicted in Fig. 2.2. The first phase is the CA for minimizing the interference among WLAN basic service sets (BSSs) while fully exploiting channel sharing and channel bonding. The second phase is the UA-LB for associating each STA with a pair of AP and band-channel (i.e., which band channel of which AP) for given CA result of the first phase, so that the network load is well balanced among assigned channels of APs. Since the load balancing in this UA work means the load balancing among assigned channels (not among APs),

hereafter, this second phase is denominated as UA-ChLB rather than UA-LB. Now, we give a short overview of each RRM phase.

2.2.1 Channel Assignment

As depicted in Fig. 2.2, the CA task is composed of three sub-tasks: generating the interference graph among APs, allocating the operation channel and its bandwidth to each AP, and selecting the primary channel among the allocated basic channels of each AP. Now, we explain each subtask, using our previous work in [9]. Since the CA scheme in [9] was designed under the same system model as that in the thesis, this scheme is well matched to the CA part of Fig. 2. Accordingly, we summarize the CA scheme in [9] without newly designing another CA scheme, in this subsection.

Interference Graph Generation

The graph generation process in [9] is as follows, separately for each band. The controller requests C-APs to search the neighboring S-APs (i.e., stand-alone APs) by scanning all channels. Then, each C-AP can detect its directly interfering S-APs and get the operating channel information of neighboring S-APs. Next, the controller makes a beacon broadcasting schedule of each C-AP in time-division manner. A C-AP broadcasts beacon frame at its scheduled time, on a predefined channel. Then, other C-APs can observe its direct interference relationship with the C-AP by listening to the broadcasted beacon. After that, according to reporting schedule, each C-AP reports its interfering C-APs and S-APs to the controller (of course, also the channel number of each neighboring S-AP). From this reported information, the controller can acquire direct interference relationship among all

16

APs, including C-APs and S-APs.

On the other hand, similarly to C-APs, each NL-STA also detects its directly interfering S-APs and C-APs and reports the list to the controller. It is noted that, based on this reported information, the controller can get the hidden interference relationship among APs. For example, if there is no direct relationship between AP-k and AP-l but there is an NL-STA having direct interference relationship with both AP-l and AP-k, respectively, then the AP-k and AP-l are hidden interferer to each other.

By using the reported information from C-APs and NL-STAs, the controller generates the weighted interference graph, where APs (both C-APs and S-APs) become the vertexes and the interfering APs are connected with edges. The weight of an edge depends on whether the interference relationship of the edge is direct or hidden: the weight of a direct interference edge is set to 1, and the weight of hidden interference edge from AP-k to AP-l is set to $\frac{N_{k,l}}{N_k}$, where N_k is the number of STAs which can hear AP-k and $N_{k,l}$ is the number of STAs which can hear both of AP-k and AP-l. Then, the weight represents the probability of channel sharing between AP-k and AP-l when assigning the same channel to them.

Channel and Bandwidth Allocation

After generating interference graphs, the controller performs channel and bandwidth allocation for each C-AP.

Let $\mathcal{W}_B$ denote the set of all feasible channels for allocation, in band $B \in \{2.4, 5\}$ GHz. Since the channel bonding is allowed for each band, all channels in $\mathcal{W}_B$ do not have the same bandwidth. For example, when bonding two basic channels of 2.4 GHz band, the bonded channel becomes another 2.4 GHz-channel with 40 MHz

bandwidth. Thus, the bandwidth of a channel can be naturally identified by the channel itself. As a result, channel allocation includes bandwidth allocation.

The goal of CA in [9] is to allocate the channels so as to maximize the total throughput of entire network, while allowing channel sharing. Note that, since each AP supports dual-band, one channel in each of two bands can be assigned to an AP. Thus, the controller performs the following channel and bandwidth allocation work, separately for each band. We will omit the band index B for convenience in description.

When c_k denotes a channel allocated to AP-k, channel allocation is represented as $(c_1, c_2, \cdots, c_K)$ where K is the number of C-APs. Since the same channel or overlapped channels can be allocated to two APs having interference relationship, the maximum throughput of each AP is affected by such channel sharing. For given $(c_1, c_2, \cdots, c_K)$ and the channels of S-APs, the channel sharing factor of each C-AP is calculated based on the weighted interference graph, which is to add all weights of interference edges of the C-AP for the corresponding channel allocation. Then, the maximum throughput of a C-AP under channel sharing is got by dividing its maximum throughput under no sharing by its channel sharing factor. The CA work is formulated as the optimization problem for maximizing the throughput sum of all C-APs.

Primary Channel Selection

As the final subtask, the controller determines the primary basic channel of each bonded channel for given CA result. Note that IEEE 802.11ac standard supports two strategies of using the bonded channel: the static strategy is to always use the whole allocated basic channels for every transmission, whereas the dynamic strategy

18

allows AP and STAs to use just free contiguous basic channels including primary channel. According to [8], for static bonding strategy, two types of channel invading can also occur among two adjacent APs using the same channel: total invading where one AP always wins in channel access, and a partial invading where one AP has the lower channel access opportunity than the other AP. Under invading situation, note that the primary channel section may have a great effect on the performance.

In [9], the controller selects the primary channel for bonded channel of each C-AP, while taking bonding strategy and invading type into account. More specifically, if AP-k and AP-l have total invading relation, their primary channels should be set on the same basic channel. Otherwise, i.e., for partial invading or dynamic channel bonding case, their primary channels should be set to different basic channels which are farthest away from each other.

The readers can refer to [9] for the detail of the CA scheme, summarized above.

2.2.2 User Association for Balancing Load on Channels

The controller periodically performs the UA-ChLB work, based on various status information reported from all NL-STAs and C-APs. Since the state of STAs (traffic, location, etc) may be changed dynamically, it can be better to carry out the UA-ChLB more often, in the viewpoint of performance. But, this may incur a considerable reporting overhead. That is, there is a trade-off between performance and communication overhead. To properly handle this trade-off, we propose the hybrid scheme, composed of distributed UA-ChLB and centralized UA-ChLB. The centralized UA-ChLB is carried out by the controller with longer period and the distributed UA-ChLB is performed independently by each STA, at any time.

19

On the other hand, the CA work can be performed with much longer period than the centralized UA-ChLB since interference relationship among APs (mainly influenced by positions of APs) is expected to be not greatly changed over time.

As already stated before, since the CA scheme [9] can be used for the CA part of Fig. 2, we will concentrate on designing the centralized UA-ChLB and the distributed UA-ChLB, under situation that the operating channels of each C-AP have been determined already by the CA scheme [9].

2.3   Hybrid UA-ChLB

In the proposed UA-ChLB, the controller performs the UA task (i.e., determines serving AP and operating channel within the serving AP) for NL-STAs with period of T_{UA}. This work is referred to as the centralized UA-ChLB by the controller. It is noted that an NL-STA can be associated with S-AP if the NL-STA is expected to get better transmission opportunity from the S-AP than C-APs, for example, when the NL-STA is very close to the S-AP or the load of S-AP is low. On the other hand, the network status can be greatly changed during the interval of centralized UA-ChLB work. To efficiently cope with such fluctuation of network status with low overhead, we take a strategy to adjunctively use the distributed UA-ChLB during the interval of centralized UA-ChLB. In the distributed UA-ChLB, each NL-STA can change its serving AP and/or the serving channel, at any time if the predefined condition for such handover is held.

2.3.1 Distributed UA-ChLB

Consider an NL-STA-i associated with the band-B channel of AP-k, where the AP-k can be C-AP or S-AP. Remind that AP-k, irrespective of C-AP or S-AP, broadcasts $[L(k,B), |\mathcal{S}(k,B)|, \Gamma(k,B)]$ for each band-B, through its beacon frames, where $L(k,B)$, $|\mathcal{S}(k,B)|$, and $\Gamma(k,B)$ are the total load, the number of associated STAs, and the SE for band-B channel in AP-k, respectively.

When getting $[L(k,B), |\mathcal{S}(k,B)|, \Gamma(k,B)]$, the NL-STA-$i$ checks whether $L(k,B)$ is higher than a predefined threshold value L_{th}. If $L(k,B) > L_{\text{th}}$, the STA-i conducts a persistent test with the probability of $\frac{1}{|\mathcal{S}(k,B)|}$. When the persistent test is passed, the NL-STA-i performs the following task which determines the target AP and band for handover.

Firstly, the NL-STA-i gets the information of neighboring APs by hearing beacon frames through the full channel scanning process. Next, for each channel of all neighboring APs, the NL-STA-i assesses the average SE of channel when it is associated with the corresponding channel, as follows. Let $\Gamma_i(j,B)$ be the average SE for the band-B channel of AP-j assessed by NL-STA-i (refer to the equations (2.3), (2.4)). Since the NL-STA-i is newly added,

$$\Gamma_i(j,B) = \frac{1 + |\mathcal{S}(j,B)|}{\frac{1}{f(SNR_{j,i})} + \frac{|\mathcal{S}(j,B)|}{\Gamma(j,B)}}, \tag{2.5}$$

where $SNR_{j,i}$ is the SNR of AP-j at NL-STA-i measured by hearing the beacon of AP-j. On the other hand, it is obvious that the resource efficiency (RE) of this new assigned NL-STA-i on the band-B channel of AP-j is affected by not only the existing load of AP-j but also the loads of neighboring APs of NL-STA-i on the corresponding channel. It is obvious that the higher load leads to the lower RE. Thus, when the NL-STA-i is newly associated with the band-B channel of AP-j,

$$L(k, B) = \hat{L}(k, B) + \sum_{i \in \hat{S}_{\text{CSTA}}} x_i(k, B) \frac{\alpha_i}{C_{k,i}} - y_{\text{C-AP}}(k) \sum_{n \in \hat{S}_{\text{CSTA}}(k,B)} \frac{\alpha_n}{C_{k,n}}. \quad (2.9)$$

$$\Gamma(k, B) = \frac{\left|\hat{S}(k, B)\right| + \sum_{i \in \hat{S}_{\text{CSTA}}} x_i(k, B) - y_{\text{C-AP}}(k) \left|\hat{S}_{\text{CSTA}}(k, B)\right|}{\frac{\left|\hat{S}(k,B)\right|}{\hat{\Gamma}(k,B)} + \sum_{i \in \hat{S}_{\text{CSTA}}} \frac{x_i(k,B)}{f(SNR_{k,i})} - y_{\text{C-AP}}(k) \sum_{n \in \hat{S}_{\text{CSTA}}(k,B)} \frac{1}{f(SNR_{k,n})}} (2.10)$$

the expected RE of NL-STA-i, $RE_i(j, B)$, is likely to be inversely proportional to the total load of the channel. Let $\mathcal{A}_i(j, B)$ be the set of neighboring APs of NL-STA-i using the band-B channel of AP-j and let $\mathfrak{L}_i(j, B)$ denote the total load for band-B channel of AP-j being estimated by NL-STA-i. Because the load of NL-STA-i should be added,

$$\mathfrak{L}_i(j, B) = \frac{\alpha_i}{C_{j,i}} + \sum_{m \in \mathcal{A}_i(j,B)} L(m, B). \quad (2.6)$$

Then, the decreasing factor of RE is defined as $\beta_i(j, B) := \frac{1}{1+\mathfrak{L}_i(j,B)}$, where we add 1 to $\mathfrak{L}(j, B)$ in the denominator so that $\beta_i(k, B)$ has a real positive value such that $0 < \beta_i(k, B) \leq 1$. And, the NL-STA-i estimates the RE for the band-B channel of AP-j, as follows.

$$RE_i(j, B) := \beta_i(j, B) \cdot \Gamma_i(j, B). \quad (2.7)$$

The NL-STA-i determines the target AP-j^* and band-B^* as

$$(j^*, B^*) = \underset{j \in \mathcal{A}_i(j,B), B \in \{2.4 \text{ GHz}, 5 \text{ GHz}\}}{\operatorname{argmax}} RE_i(j, B). \quad (2.8)$$

2.3.2 Centralized UA-ChLB

Remind that an AP being governed by the controller is called C-AP and the STA where the proposed UA-ChLB is implemented is called NL-STA. Since the con-

troller only manages the C-APs, it receives the information from both C-APs and the NL-STAs connected to C-APs (i.e., C-STAs).

The controller performs the UA for all C-STAs with the period of T_{UA}. Since a C-STA can be associated with not only C-AP but also S-AP, the UA should estimate the link rate between the C-STA and its each neighboring AP. Since the link rate is calculated based on the link quality (i.e., SNR value), the controller requests all C-STAs to search their neighboring S-APs by scanning channels.[1] In addition, since the controller knows channels assigned to C-APs, it provides the channel information of neighboring C-APs to C-STAs, through their current serving C-APs. Each C-STA, by hearing the beacons of its neighboring S-APs and C-APs for each band, measures the SNR of beacon and gets the information within beacon. Then, it reports the list of neighboring APs and the information within beacon and SNR of beacon for each neighboring AP. Remind that any AP, irrespective of C-AP or S-AP, broadcasts a beacon containing the number of associated STAs, the channel load, and the average SE, for each band channel. The controller also directly gets the information for UA from each C-AP, i.e., the list of associated STAs, the traffic arrival rate of each C-STA, the channel load, and the SE for each band channel.

The controller determines the serving AP and serving channel of each C-STA for maximizing the total RE of entire network, based on the above information reported from C-APs and C-STAs. We firstly formulate the centralized UA-ChLB work as a mixed-integer quadratic fractional programming (MIQFP) problem, which can be transformed into a mixed-integer quadratic programming (MIQP). Then, we get

---

[1] Although full channel scanning is performed in the CA process, since the period of CA is much longer than T_{UA}, the information on neighboring S-APs may be changed.

the UA result by solving the transformed MIQP problem.

Problem Formulation

We define notation for the information that the controller gathers at the start of the centralized UA-ChLB process, as follows. Let $\hat{S}_{\text{CSTA}}$ denote the set of NL-STAs connected to all C-APs. For the band-B channel of AP-k, let $\hat{S}(k, B)$ be the set of all associated STAs and let $\hat{S}_{\text{CSTA}}(k, B)$ be the set of associated C-STAs. When $y_{\text{C-AP}}(k)$ is a binary variable indicating whether the AP-k is C-AP or not, if the AP-k is C-AP, $y_{\text{C-AP}}(k) = 1$; otherwise, $y_{\text{C-AP}}(k) = 0$. Obviously, if $y_{\text{C-AP}}(k) = 0$, $\hat{S}_{\text{CSTA}}(k, B) = \emptyset$.

We represent a feasible UA result as a matrix $\mathbf{X} := [x_i(k, B)]$, where $x_i(k, B)$ is a binary variable indicating whether C-STA-i is associated with the band-B channel of AP-k or not. This is, if the C-STA-i is associated with the band-B channel of AP-k, $x_i(k, B) = 1$; otherwise, $x_i(k, B) = 0$.

As mentioned before, the controller tries to maximize the total RE of entire network, which is the sum of the REs of all APs. Similarly in the distributed UA-ChLB of the previous subsection, we define the RE for the band-B channel of AP-k as the channel SE multiplied by the decreasing factor which is inversely proportional to the load.

Firstly, let us estimate the load for the band-B channel of any AP-k, denoted by $L(k, B)$. When $\hat{L}(k, B)$ denotes the load on the band-B channel of AP-k got from the beacon of AP-k at the start of the current centralized UA-ChLB process, $L(k, B)$ is estimated as (2.9). Since the controller re-associates only the NL-STAs within C-APs, if AP-k is S-AP (i.e., $y_{\text{C-AP}}(k) = 0$), the estimated load for the band-B channel of AP-k is the sum of its existing load and the loads of newly associated

NL-STAs among the STAs in $\hat{S}_{\mathrm{CSTA}}$. And, if AP-k is C-AP, the load of its past associated NL-STAs should be additionally subtracted. Since the channel sharing is allowed, the load on the band-B channel of AP-k should be assessed by counting the loads of neighboring APs using the same channel together. Accordingly, the total load on the band-B channel of AP-k is estimated as

$$\mathfrak{L}(k, B) := \sum_{j \in \{k\} \cup \mathcal{A}(k,B)} L(j, B), \tag{2.11}$$

where $\mathcal{A}(k, B)$ be the set of neighboring APs of AP-k, sharing the band-B channel of AP-k. Then, since the higher $\mathfrak{L}(k, B)$ means that the AP-k may occupy the smaller portion of channel time, the RE for the band-B channel of AP-k is expected to be lower for higher $\mathfrak{L}_{(}k, B)$. Thus, we set the decreasing factor $\beta(k, B)$ as a real positive value being proportional to the reciprocal of $\mathfrak{L}(k, B)$.

$$\beta(k, B) = \frac{1}{1 + \mathfrak{L}(k, B)}. \tag{2.12}$$

Note that $0 < \beta(k, B) \leq 1$, by adding 1 to the denominator.

On the other hand, the estimated average SE for band-B channel of AP-k, denoted by $\Gamma(k, B)$, is defined as a harmonic mean of the SEs of associated STAs. In (2.10), $f(SNR_{k,i})$ is the SE between STA-i and AP-k (refer to (2.3)) and $\hat{\Gamma}(k, B)$ is the average SE for the band-B cannel of AP-k got by hearing the beacon of AP-k at the start of the current centralized UA-ChLB process. Note that the numerator of (2.10) is the total number of STAs and its denominator is the sum of the reciprocals of SE for all STAs.

The controller calculates the RE of AP-k on its band-B channel, denoted by $RE(k, B)$, as follows.

$$RE(k, B) := \beta(k, B) \cdot \Gamma(k, B). \tag{2.13}$$

Then, the optimization problem for centralized UA-ChLB, which maximizes the RE of entire network, can be formulated as (2.14) and the solution is the new AP/channel association for each STA in $\hat{S}_{\text{CSTA}}$.

$$\max_{\mathbf{X}} \sum_{(k,B)\in\mathcal{C}} RE(k,B) \tag{2.14}$$

$$s.t. \sum_{(k,B)\in\mathcal{C}} x_i(k,B) = 1, \quad \forall i \in \hat{S}_{\text{CSTA}}, \ \forall (k,B) \in \mathcal{C} \tag{2.15}$$

$$x_i(k,B) \in \{0,1\}, \qquad \forall i \in \hat{S}_{\text{CSTA}}, \ \forall (k,B) \in \mathcal{C} \tag{2.16}$$

$$\mathfrak{L}(k,B) \leq L_{\text{th}}, \qquad \forall (k,B) \in \mathcal{C} \tag{2.17}$$

where $\mathcal{C}$ is the set of which each component is a pair of each AP and its assigned channel, and is given as the input of this UA-ChLB process. It is noted that the controller knows the assigned channels of C-APs because it performs the CA work and it also knows the channel information of each S-AP because C-STAs report the channel information for their neighboring S-APs.

The constraint (2.15) is to ensure that each C-STA is associated with just an AP and one channel of the AP, and the constraint (2.16) is self-evident. The constraint (2.17) is the maximum load condition that $\mathfrak{L}(k,B)$ should be less than a predefined threshold L_{th}.

Equivalent MIQP Problem

Since the objective function (2.14) has a fractional form, this problem is an MIQFP problem, which is the NP-hard being difficult to solve directly. Therefore, we transform this original problem into an equivalent solvable MIQP problem.

According to a parametric technique in [25], by introducing additional variables (i.e., parameters), an MIQFP problem of fractional form can be transformed into its

equivalent MIQP problem of quadratic form. We introduce the parameter $\lambda(k, B)$ for each $(k, B) \in \mathcal{C}$. For simple description, let us denote the numerator and the denominator of average SE in (2.10) by $\Gamma_{\mathrm{nu}}(k, B)$ and $\Gamma_{\mathrm{de}}(k, B)$, respectively. Then, the problem in (2.14) – (2.17) is transformed into the following MIQP problem.

$$\max_{\mathbf{X}} \sum_{(k,B) \in \mathcal{C}} \Big(\beta(k, B) \Gamma_{\mathrm{nu}}(k, B) - \lambda(k, B) \Gamma_{\mathrm{de}}(k, B) \Big) \tag{2.18}$$

$$s.t. \sum_{(k,B) \in \mathcal{C}} x_i(k, B) = 1, \quad \forall i \in \hat{S}_{\mathrm{CSTA}}, \ \forall (k, B) \in \mathcal{C} \tag{2.19}$$

$$x_i(k, B) \in \{0, 1\}, \quad \forall i \in \hat{S}_{\mathrm{CSTA}}, \ \forall (k, B) \in \mathcal{C} \tag{2.20}$$

$$\mathfrak{L}(k, B) \leq L_{\mathrm{th}}, \quad \forall (k, B) \in \mathcal{C} \tag{2.21}$$

For given $\lambda(k, B)$'s, the MIQP problem in (2.18) – (2.21) can be solved by applying the branch and bound (BB) technique. By using the CPLEX MIQP solver[2] [26], we obtain the solution for given $\lambda(k, B)$'s.

Solution Algorithm

The solution of original problem, $\mathbf{X}^*$, is obtained by solving the transformed problem in (2.18) – (2.21) with the optimal values of $\lambda(k, B)$'s for maximizing the objective function (2.18). It is well known that these optimal parameter values, $\lambda(k, B)^*$'s, can be got by applying the Dinkelbach's method [27]. According to the Dinkelbach's method, each $\lambda(k, B)$ is initially set to 0, and its value is repeatedly updated and finally converges to $\lambda^*(k, B)$.

Algorithm 1 is the solution algorithm of centralized UA-ChLB problem, based on the Dinkelbach's method. The algorithm is terminated when all parameters

---

[2]There are actually plenty of solvers which use the BB technique to solve MIQP problems, including CPLEX.

converge to their respective optimal values, i.e., when the gap between the old and new values is not larger than a predefined threshold ϵ.

Algorithm 1 Solution Algorithm of Centralized UA-ChLB

$\lambda(k, B) \leftarrow 0, \ \lambda^{old}(k, B) \leftarrow 1 \ \text{ for all } (k, B) \in \mathcal{C}.$

$\epsilon \leftarrow 10^{-5}, \ \text{stop} \leftarrow \text{false.}$

while stop $=$ *false* **do**

    Solve the problem $(2.18) - (2.21)$, for given $\lambda(k, B)$'s

    stop $\leftarrow$ *true*

    for all $(k, B) \in \mathcal{C}$ **do**

        if $\left| \lambda(k, B) - \lambda^{old}(k, B) \right| > \epsilon$ **then**

            $\lambda^{old}(k, B) \leftarrow \lambda(k, B)$

            Calculate$RE(k, B)$ by using Eq. (2.13)

            $\lambda(k, B) \leftarrow RE(k, B)$

            stop $\leftarrow$ *false*

        end if

    end for

end while

return $\mathbf{X}^{*}$

Remark: The NL-STAs which were associated with C-APs are newly associated with C-AP or S-AP, based on the centralized UA-ChLB result. During the interval of the centralized UA-ChLB, since each NL-STA can change its serving AP and serving channel whenever the condition for handover is satisfied, the proposed scheme has the desirable properties, which are the efficiency of centralized allocation and the fast adaptation of distributed control.

Chapter 3. Time Resource Management in UWB Ranging System

3.1 IEEE 802.15.4z Ranging Operation

3.1.1 Basic Ranging Concept

For simple description, we consider any two RDEVs named as RDEV-A and RDEV-B, respectively. As depicted in Fig. 3.1, the ToF between RDEV-A and RDEV-B can be estimated through the exchange of an initiation message (IM) and a response message (RM) between them, i.e., two-way ranging. There are two types of two-way ranging: a single-sided two-way ranging (SS-TWR) and a double-sided two-way ranging (DS-TWR).

In the SS-TWR, the RDEV-A sends an IM to the RDEV-B, and the RDEV-B replies by sending an RM to the RDEV-A. Let T_{reply} be the duration between the receiving time of the IM and the sending time of the RM, at the RDEV-B. And, let T_{round} be the round trip delay between the sending time of the IM and the receiving time of the RM, at the RDEV-A. The RM from RDEV-B to RDEV-A includes T_{reply} measured by the RDEV-B. When receiving the RM, the RDEV-A can estimate the ToF in the SS-TWR as $\hat{T}_{\text{prop}} = \frac{T_{\text{round}} - T_{\text{reply}}}{2}$.

For better ToF estimation, the DS-TWR repeats this SS-TWR twice, alternately once at each side (i.e., RDEV-A, RDEV-B). In the DS-TWR, let T_{reply1} and T_{reply2} be the durations between the receiving time of an IM and the sensing time of the corresponding RM, at the RDEV-B and the RDEV-A, respectively. And, let T_{round1} and T_{round2} are the round trip delays at the RDEV-A and the RDEV-B, respectively (see Fig. 3.1). Then, the ToF in the DS-TWR can be esti-
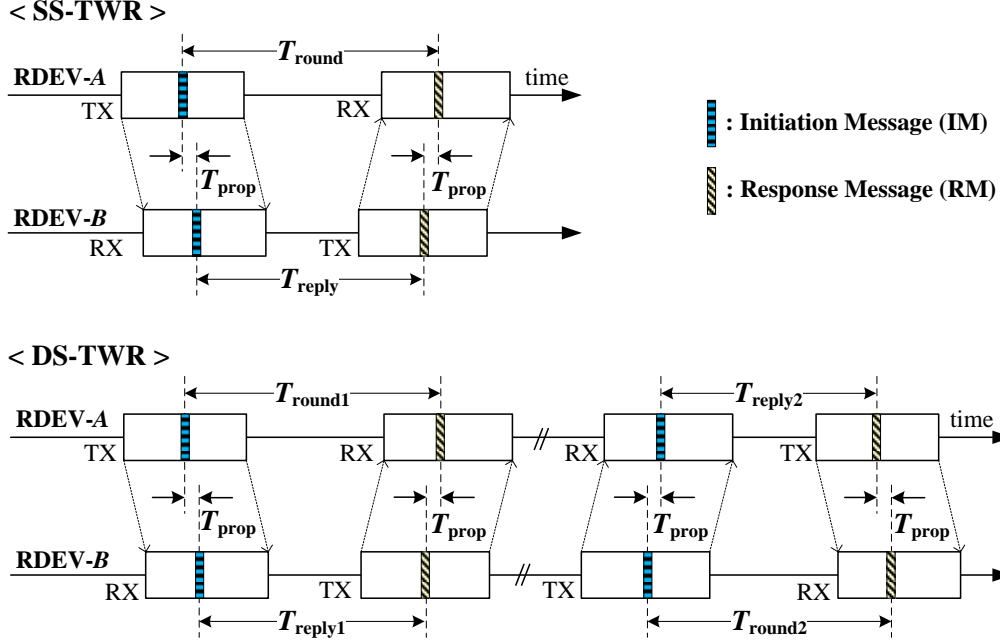
< SS-TWR >

< DS-TWR >

Fig. 3.1: SS-TWR and DS-TWR

mated as $\hat{T}_{\text{prop}} = \frac{T_{\text{round1}} \cdot T_{\text{round2}} - T_{\text{reply1}} \cdot T_{\text{reply2}}}{T_{\text{round1}} + T_{\text{round2}} + T_{\text{reply1}} + T_{\text{reply2}}}$ [47].

3.1.2 RDEV Types and Ranging Phases

The IEEE 802.15.4z defines four types of RDEVs: controller, controlee, initiator, and responder. Within a ranging group, there exists a single controller which broadcasts a ranging control message (RCM), and multiple controlees which receive the RCM. The RDEVs can be also categorized as initiator or responder. An RDEV which initiates the ranging by sending an IM is called an initiator, whereas an RDEV which replies with an RM becomes a responder.

The RCM includes several information elements for conveying ranging parameters and scheduling information. The core ranging parameter is the information on the ranging time structure. All RDEVs in a ranging group conduct the ranging
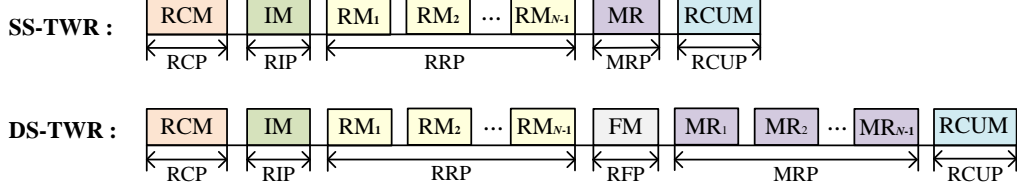
Fig. 3.2: Ranging phases of SS-TWR and DS-TWR in IEEE 802.15.4z
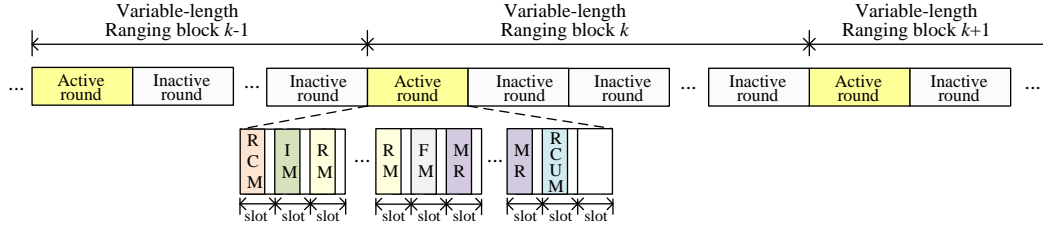
Fig. 3.3: Ranging time structure for IEEE 802.15.4z ranging devices in the proposed scheme

process according to this ranging time structure. We will explain the ranging time structure while describing the ranging process in the next subsection. On the other hand, the scheduling information in the RCM indicates when each controlee sends or receives ranging messages according to its role as initiator or responder.

To support various ranging conditions, the IEEE 802.15.4z defines three modes depending on the numbers of initiator(s) and responder(s): one-to-one, one-to-many, and many-to-many modes. This mode information is included in the RCM. In this paper, we focus on the one-to-many mode where there are one initiator and multiple responders in a ranging group, because this mode is expected to be mainly used for highly precise localization.

Fig. 3.2 shows the ranging phases of SS-TWR and DS-TWR in the one-to-

many mode, where a ranging group is composed of one initiator and $(N - 1)$ responders. In the SS-TWR, one entire *range measuring cycle* consists of five phases: the ranging control phase (RCP), the ranging initiation phase (RIP), the ranging response phase (RRP), the measurement report phase (MRP), and the ranging control update phase (RCUP). Whereas, in the DS-TWR, one entire range measuring cycle has six phases and, as shown in Fig. 3.2, the ranging final phase (RFP) is added and multiple measurement reports are conducted in the MRP.

Let us describe each ranging phase focusing on the DS-TWR. A controller broadcasts the RCM in the RCP, and an initiator sends an IM to other responders in the RIP. Then, each responder replies to the initiator by sending its RM in the RRP. The initiator sends a final message (FM) to the responders in the RFP, and each responder sends a measurement report (MR) to the initiator. Finally, in the RCUP, the controller broadcasts a ranging control update message (RCUM), which updates the ranging parameters and indicates when the next range measuring cycle is started.

3.1.3 Ranging Time Structure

In IEEE 802.15.4z, the channel time is divided by the ranging blocks and a ranging block is composed of N_{round} ranging rounds.[1] Each ranging round is the time period enough to complete one entire range measuring cycle in Fig. 3.3, irrespective of whether the ranging type is the SS-TWR or DS-TWR. A ranging round is furthermore subdivided into N_{slot} ranging slots and each ranging slot is enough to transmit one ranging message (such as RCM, IM, RM, FM, MR, or RCUM in

---

[1]For readability, one can refer to Fig. 3.3 depicting a ranging time structure of the proposed scheme, since the proposed scheme is designed to comply with IEEE 802.15.4z.

Fig. 3.2). The length of a ranging slot, L_{slot}, is specified by an integral multiple of a ranging scheduling time unit (RSTU) which is the smallest time unit in the MAC. For the high rate pulse repetition frequency UWB PHY, one RSTU is equal to 833.33 ns. When L_{round} denotes the length of a ranging round, $L_{\text{round}} = N_{\text{slot}} \times L_{\text{slot}}$. Then, the length of a ranging block is $L_{\text{block}} = N_{\text{round}} \times L_{\text{round}}$.

According to IEEE 802.15.4z, there exists a single active round within each ranging block and the remaining rounds are inactive. The RDEVs conduct the ranging process in only the active round and sleep in all inactive rounds for energy saving. Accordingly, since the RDEVs have an opportunity of obtaining the ranging results merely once every ranging block, the block length corresponds to the ranging interval. The ranging block length is a very important factor having a great influence on both the ranging delay and energy efficiency of the corresponding ranging group.

3.1.4   Ranging Block Length

The ranging process within a group is governed by the controller of the group. That is, for every ranging block, the controller selects an initiator, makes a schedule for the message sending time of each responder (i.e., RRP and MRP in Fig. 3.2), and also determines the length of the block. At the start of the active ranging round of each block, the controller notifies the block length and the scheduling information to the controlees, by broadcasting the RCM.

The RDEVs may prefer the different block lengths, according to their respective application characteristics. When an RDEV wants to change the length of the next ranging block to its preferred value, it sends a ranging parameter update message (RPUM) which contains its preferred block length. According to the in-band

33

signaling manner complying with the IEEE 802.15.4z standard, each responder can send the RPUM with its response or report message together (RM and MR of the active round) within the current ranging block. The initiator also can send its RPUM during the RIP or RFP of the active round (see Fig. 3.2). Based on the update requests received during the current block, the controller should determine the length of the next block appropriately. For a given ranging block length, the time synchronization among RDEVs in a ranging group should be conducted to provide a highly accurate ranging among them. To do this, RCM and RCUM transmitted by the controller are utilized see Fig. 3.3). Through these messages, the RDEVs in the ranging group maintain the synchronization with the decided ranging block structure while being idle with its receiver turned off during unused ranging slots to save energy.

In the following section, we design a block length decision scheme for IEEE 802.15.4z UWB ranging devices.

3.2   Proposed scheme

3.2.1   System Model

Let us consider a small-scale ranging group of N RDEVs, composed of a controller and $(N - 1)$ controlees. These RDEVs conduct the DS-TWR according to an one-to-many mode having an initiator and $(N - 1)$ responders.

In the proposed scheme, the length of a ranging block is variable and, a round length and a slot length are fixed.[2] Thus, the number of ranging rounds within a

---

[2]As stated earlier, all messages in the DS-TWR should be able to be sent during one round and a slot time should have a sufficient length to send any ranging message. Since the maximum

block represents the length of the corresponding block. On the other hand, in the proposed scheme, the active round of each ranging block is always placed at the first of the block. In actual, according to the IEEE 802.15.4z standard, the controller can change the position of the active round within a block, by assigning a different round offset for each ranging block. This is for avoiding the consecutive collisions with other neighboring groups transmitting at the same time. However, like in the proposed scheme, when the ranging block length is changed at each block, although the active round of each ranging block is always placed at the first of the block, a similar effect can be obtained. Thus, we design the proposed scheme so that each block starts with the active round for ranging operation. Fig. 3.3 depicts a ranging time structure under the proposed scheme.

Without loss of generality, we assume that each RDEV has its preferred block length and the preferred block lengths of the RDEVs can be different from each other. If an RDEV has a block length update request at the start of an active round, the RDEV transmits its update request during the corresponding active round.

At the start of each ranging block, the controller decides the length of the corresponding block while referring to the length update requests received during the previous block, and notifies the decided block length to the RDEVs through the RCM. Upon receiving the RCM, an RDEV can know whether its request at the previous block has been accepted or not. When the current block length is equal to its preferred length, the RDEV does not send any update request during the current block, since it has already been satisfied and has no need for update. If

number of RDEVs within a ranging group is typically pre-defined, note that it is reasonable to fix a round length and a slot length to their respective allowable maximum values.

the block length is not set to its preferred block length, the RDEV again transmits its update request during the active round of the current ranging block.

3.2.2   MDP-Based Block Length Decision

It is well known that MDP provides a mathematical framework for modeling decision-making in situations where outcomes are partly random and partly under the control of the decision maker. Within an UWB ranging group under consideration, the controller is a decision maker which determines the ranging block length, based on the update requests from the controlee RDEVs. Since the RDEVs generate their respective update requests independently of each other, the request generation within the ranging group has a property of randomness. Therefore, the block length decision process can be very appropriately designed by using an MDP. For this reason, in this paper, we adopt an MDP framework as a design tool for deciding a ranging block length.

Let us assume that, when an RDEV-n has no request waiting for transmission, the elapsed time until an arrival of a new length update request is randomly determined according to an exponential distribution of mean $1/\lambda_n$. Note that λ_n corresponds to a new request arrival rate of the RDEV-n. Then, we can formulate the block length decision process of the controller as a discrete-time MDP, where the start time of each ranging block is a decision epoch and the MDP state at a decision epoch is represented with the previous block length and the update requests sent at the previous block.

In general, an MDP is defined as a four-tuple $< \mathcal{S}, \mathcal{A}, \mathcal{P}, \mathcal{R} >$, where $\mathcal{S}$ is a state space, $\mathcal{A}$ is an action space, $\mathcal{P}$ is a state transition probability matrix, and $\mathcal{R}$ is a real valued reward function. Let us define each component of the proposed

MDP.

States

Let x_n be a binary indicator representing whether an RDEV-n sent a block length update request during the previous block. It is noted that the update requests generated during the previous block are sent during the active round of the current block and these are reflected as the next state. Since a request generation depends on the length of the corresponding block, we take the previous block length as one component of a state. Let b_p be the length of the previous ranging block. Then, the system state is defined as $\mathbf{s} = (b_p, x_1, x_2, \cdots, x_N)$, where N is the number of RDEVs.

Suppose that there are M different preferred lengths, $\ell_1, \cdots, \ell_M$, from N RDEVs within the same group. Since each RDEV is assumed to have one preferred block length and some RDEVs can have the same preferred length, $M \leq N$. Let $g(\cdot)$ denote a mapping function between the index of an RDEV and the preferred block length of the RDEV. For example, if the preferred block length of an RDEV-n is ℓ_i, $g(n) = \ell_i$. Note that the length of a ranging block is selected among the preferred lengths of the RDEVs. When $\mathcal{L}$ denotes a set of all feasible ranging block lengths, $\mathcal{L} = \{\ell_1, \ell_2, \cdots, \ell_M\}$.

Then, the state space $\mathcal{S}$, i.e., a set of all feasible states is
$$\mathcal{S} = \{(b_p, x_1, x_2, \cdots, x_N) \mid b_p \in \mathcal{L}, x_n \in \{0, 1\}, 1 \leq n \leq N\}.$$

Actions

Let $\mathcal{A}_{\mathbf{s}}$ be a set of allowable actions at a state $\mathbf{s}$. The action space, $\mathcal{A}$, is expressed as $\mathcal{A} = \bigcup_{\mathbf{s} \in \mathcal{S}} \mathcal{A}_{\mathbf{s}}$. Let a_i represent an action to choose ℓ_i as a ranging block

length. In other words, the action a_i is mapped to the ranging block length ℓ_i. Since the controller selects a ranging block length among the elements of $\mathcal{L}$, $\mathcal{A} = \{a_1, a_2, \cdots, a_M\}$.

State Transition Probability

Let $p(\mathbf{u}|\mathbf{s}, a_i)$ be the probability that, when an action a_i is chosen at the current state $\mathbf{s}$, the system transits to the state $\mathbf{u}$ at the next decision epoch. Let $\mathbf{s} := (b_p, x_1, x_2, \cdots, x_N)$ and $\mathbf{u} := \left(\hat{b}_p, \hat{x}_1, \hat{x}_2, \cdots, \hat{x}_N\right)$. Since a_i is mapped to ℓ_i, it is obvious that $\hat{b}_p$ should be ℓ_i. Thus, when $\hat{b}_p \neq \ell_i$, $p(\mathbf{u}|\mathbf{s}, a_i) = 0$.

Note that the RDEVs are independent from each other. Thus, for the transition from a system state $\mathbf{s}$ to another system state $\mathbf{u}$, the next state $\hat{x}_n$ of any RDEV-n depends on only its current state x_n, the previous block length b_p, and the action a_i, and is not influenced by the current and next states of other RDEVs. Let $f_n(b_p, a_i)$ be the probability that the state of an RDEV-n transits from x_n to $\hat{x}_n$, for given previous block length b_p and action a_i. Because of such independence among RDEVs, we can express the probability that a system state transits from $\mathbf{s} = (b_p, x_1, x_2, \cdots, x_N)$ under the action a_i to $\mathbf{u} = \left(\hat{b}_p, \hat{x}_1, \hat{x}_2, \cdots, \hat{x}_N\right)$, as the following product form.

$$p(\mathbf{u}|\mathbf{s}, a_i) = \begin{cases} \prod_{n=1}^{N} f_n(b_p, a_i), & \text{if } \hat{b}_p = \ell_i \\ 0, & \text{if } \hat{b}_p \neq \ell_i \end{cases} \tag{3.1}$$

Now, let us derive $f_n(b_p, a_i)$. Note that the controller under the proposed scheme takes an action which leads to the maximization of the expected reward, regardless of whether the corresponding RDEV did send its request at the previous ranging block or not. That is, even when $x_n = 0$, it is possible to select the action a_i such that $\ell_i = g(n)$.

First, we examine the case such that $\ell_i = g(n)$. Then, since the RDEV-n is satisfied with the current ranging block length, although the RDEV-n has an update request waiting for transmission, it does not send the update request at the current block and discard the request. Note that the next state of the RDEV-n represents whether it has sent an update request during the current block. Thus, when $\ell_i = g(n)$, $\hat{x}_n$ should be 0, irrespective of whether $x_n = 0$ or $x_n = 1$.

Next, let us examine the case such that $\ell_i \neq g(n)$. If the RDEV-n did not send an update request at the active round of the previous block, $x_n = 0$. Then, if the RDEV-n generated a new request during the previous block, the new request is sent at the current active round and its next state $\hat{x}_n$ becomes 1. When having no request waiting for transmission, the RDEV-n generates a new request after the elapsed time randomly determined according to an exponential distribution of mean $1/\lambda_n$. Note that the probability of the elapsed time shorter than b_p (i.e., the probability that a new update request was generated during the previous block) is $1 - e^{-\lambda_n b_p}$. Accordingly, when $x_n = 0$, the RDEV-n transits to $\hat{x}_n = 1$ with probability $\left(1 - e^{-\lambda_n b_p}\right)$ or $\hat{x}_n = 0$ with probability $e^{-\lambda_n b_p}$. When $x_n = 1$, since the condition such that $g(n) \neq \ell_i$ means that the request of the RDEV-n is not accepted, the request should be transmitted again and thus $\hat{x}_n$ should be 1. In

summary,

$$
f_n(b_p, a_i) = \begin{cases}
1, & \text{if } g(n) = \ell_i,\ \hat{x}_n = 0 \\[2mm]
0, & \text{if } g(n) = \ell_i,\ \hat{x}_n = 1 \\[2mm]
e^{-\lambda_n b_p}, & \text{if } g(n) \neq \ell_i,\ x_n = 0,\ \hat{x}_n = 0 \\[2mm]
1 - e^{-\lambda_n b_p} & \text{if } g(n) \neq \ell_i,\ x_n = 0,\ \hat{x}_n = 1 \\[2mm]
0, & \text{if } g(n) \neq \ell_i,\ x_n = 1,\ \hat{x}_n = 0 \\[2mm]
1, & \text{if } g(n) \neq \ell_i,\ x_n = 1,\ \hat{x}_n = 1.
\end{cases}
\tag{3.2}
$$

Reward

Let $r(\mathbf{s}, a_i)$ denote the immediate reward when the action a_i is taken at the state $\mathbf{s}$. We design the rewards, while taking account of energy saving and satisfaction of each RDEV for the chosen action.

First, let us examine the reward from the viewpoint of energy saving. Since each ranging block has just one active round and the RDEVs keep awake only during the active round, the RDEVs can sleep longer for the longer ranging block. Thus, when the selected block length is longer than its preferred block length, an RDEV can save more energy. Based on this reasoning, when the action a_i is selected, we assess the energy saving of the RDEV-n as being linearly proportional to the difference from the selected block length to its preferred length, i.e., $\ell_i - g(n)$. Let L_{bmax} and L_{bmin} be the maximum block length and the minimum block length, respectively. The value of $\ell_i - g(n)$ is within the range of $[L_{\text{bmin}} - L_{\text{bmax}},\ L_{\text{bmax}} - L_{\text{bmin}}]$. For generality, we design the immediate reward so that each factor has a value between 0 and 1. Then, as an energy saving reward of RDEV-n for the action a_i, we take

a function $\Upsilon_{\mathrm{E}}(n, i)$ in Fig. 3.4(a). That is,

$$\Upsilon_{\mathrm{E}}(n, i) = \frac{1}{2}\left(1 + \frac{\ell_i - g(n)}{L_{\mathrm{bmax}} - L_{\mathrm{bmin}}}\right).$$
(3.3)

Then, the energy saving reward of the entire ranging group, denoted by $R_{\mathrm{E}}(\mathbf{s}, a_i)$, is

$$R_{\mathrm{E}}(\mathbf{s}, a_i) = \sum_{n=1}^{N} \Upsilon_{\mathrm{E}}(n, i).$$
(3.4)

Next, let us design the satisfaction level of the RDEV-n for the selected action a_i. The RDEV-n can be regarded as being fully satisfied when its request is accepted. Although its request is not accepted, if the difference between its preferred length $g(n)$ and the selected block length ℓ_i is small, the RDEV-n may be partially satisfied. Such the partial satisfaction may be designed as a function which decreases according to $|\ell_i - g(n)|$. The satisfaction function can be designed variously, such as linear form or step form function. When $\Upsilon_{\mathrm{S}}(n, i)$ is the satisfaction function, a linear satisfaction reward function in Fig. 3.4(b) is defined as follows:

$$\Upsilon_{\mathrm{S}}(n, i) = 1 - \frac{x_n \cdot |\ell_i - g(n)|}{L_{\mathrm{bmax}} - L_{\mathrm{bmin}}}.$$
(3.5)

Also, the step satisfaction reward function can be defined as follows:

$$\Upsilon_{\mathrm{S}}(n, i) = \frac{x_n}{L_{\mathrm{bmax}} - L_{\mathrm{bmin}}} \cdot h(n, i),$$
(3.6)

where $h(n, i)$ is the step function divided into several sections on $|\ell_i - g(n)|$ axis. When $A := L_{\mathrm{bmax}} - L_{\mathrm{bmin}}$, $\Upsilon_{\mathrm{S}}(n, i)$ can be defined as follows:

$$h(n, i) = \begin{cases} 1, & \text{if } |\ell_i - g(n)| = 0 \\ 1/4, & \text{if } 0 < |\ell_i - g(n)| \leq A/8 \\ 1/16, & \text{if } A/8 < |\ell_i - g(n)| \leq 2A/8 \\ 0, & \text{if } 2A/8 < |\ell_i - g(n)| \leq 3A/8 \\ -1/2, & \text{if } 3A/8 < |\ell_i - g(n)| \leq A \end{cases}$$
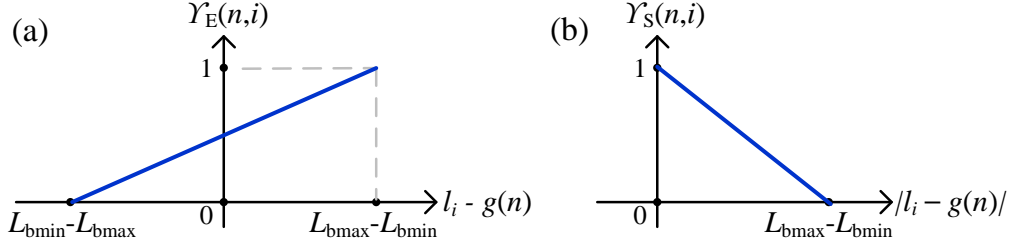(3.7)

Fig. 3.4: Design of a reward function: (a) energy saving (b) satisfaction

When $R_S(\mathbf{s}, a_i)$ denotes the satisfaction reward of the entire ranging group,

$$R_S(\mathbf{s}, a_i) = \sum_{n=1}^{N} \Upsilon_S(n, i). \tag{3.8}$$

Then, we design the immediate reward $r(\mathbf{s}, a_i)$ as

$$r(\mathbf{s}, a_i) = w\, R_E(\mathbf{s}, a_i) + R_S(\mathbf{s}, a_i), \tag{3.9}$$

where w are the relative weight of the energy saving to the satisfaction factor.

Let $J^t(\mathbf{s})$ denote the maximum possible discounted sum of rewards, being expected after t-time steps from the initial state $\mathbf{s}$.[3] When β is a discount factor, $J^t(\mathbf{s})$ is represented as

$$J^t(\mathbf{s}) = \max_{a_i \in \mathcal{A}_\mathbf{s}} \left[r(\mathbf{s}, a_i) + \beta \sum_{\mathbf{u} \in \mathcal{S}} p(\mathbf{u}|\mathbf{s}, a_i) J^{t-1}(\mathbf{u}) \right]. \tag{3.10}$$

When $\tilde{J}(\mathbf{s})$ is the converged value of $J^t(\mathbf{s})$,

$$\tilde{J}(\mathbf{s}) = \lim_{t \to \infty} J^t(\mathbf{s}). \tag{3.11}$$

---

[3]By considering that a reward in the future is not worth as much as a reward now, the expected future reward in the MDP is discounted according to the time.

Optimal Policy

Let $a^*(\mathbf{s})$ be the optimal policy in the state $\mathbf{s}$. After computing $\tilde{J}(\mathbf{u})$ for all $\mathbf{u} \in \mathcal{S}$, $a^*(\mathbf{s})$ can be obtained as follows:

$$a^*(\mathbf{s}) = \operatorname*{argmax}_{a_i \in \mathcal{A}_{\mathbf{s}}} \left[r(\mathbf{s}, a_i) + \beta \sum_{\mathbf{u} \in \mathcal{S}} p(\mathbf{u}|\mathbf{s}, a_i) \tilde{J}(\mathbf{u}) \right]. \qquad (3.12)$$

For all $\mathbf{s} \in \mathcal{S}$, the controller may calculate the best action of each state in advance for fast decision. Then, based on the current state, the controller can quickly determine the best action (i.e., selecting an optimal block length) at each decision epoch.

Chapter 4.   Performance Evaluation

4.1   Radio Resource Management Method

In this section, we assess the performances of the proposed RRM scheme and some existing schemes, based on the experimental and simulation results.

4.1.1   Implementation

We have implemented a prototype system for the proposed RRM scheme using three different entities: a centralized controller, NL-STAs, and APs (S-AP and C-AP).

Centralized Controller

The centralized controller includes a module for CA and a module for centralized UA-ChLB, which were developed by using the Java programming language (JDK version 7). For the UA-ChLB scheme, the Java version of CPLEX MIQP solver in [26] was integrated into the controller. A desktop PC using Intel i7 with 16GB RAM was used to run the controller.

NL-STAs

We used laptop computers (Samsung NT200B5C and NT500R5P) operated by Linux (Ubuntu 14.04), for NL-STAs. A wireless network interface card using Realtek 8812AU chipset is equipped to support 802.11n/ac in each laptop computer. Using the Java and iw tool (Linux), we implemented three software modules: a module for reporting wireless channel conditions and load of neighboring APs, a

module for applying its UA result notified by the controller, and a module for distributed UA-ChLB.

APs

We used TP-Link APs (TL-WDR4300, Archer C7 AC1750) operated by Open-WRT. To include the information (the number of STAs, load of AP, and average SE) in the broadcasted beacon, we modified the hostapd in the user layer without modification of Wi-Fi driver. To calculate the load of AP, the traffic amount of each STA needs to be obtained. To do this, the existing traffic monitoring tool such as *Darkstat* in each AP was exploited. Note that, through this traffic monitoring tool, the statistical information of incoming/outcoming traffic per STA can be collected. Then, the collected information is stored as a log file in the memory of each AP, and the controller can obtain the information by periodically accessing the log file.

4.1.2 Experimental Environment

We set up the experiment environment as shown in Fig. 4.1, where a total of 14 APs are deployed in rooms and corridor on the same floor of building. A total of nine APs from AP-1 to AP-9 are C-APs using 802.11n/ac (TP-Link Archer C7 AC1750) connected to the controller, whereas a total of five APs from AP-10 to AP-14 are S-APs using 802.11n (TP-Link TL-WDR4300), which independently operates. The transmission power of each AP is set to 10 dBm. To construct the dense WLAN environment where the frequency resource is insufficient, we merely use four basic channels having bandwidth of 20 MHz in each band: In 2.4 GHz band, ch.1, ch.2, ch.4, and ch.6; in the 5 GHz, ch.36, ch.40, ch.44, and ch.48.
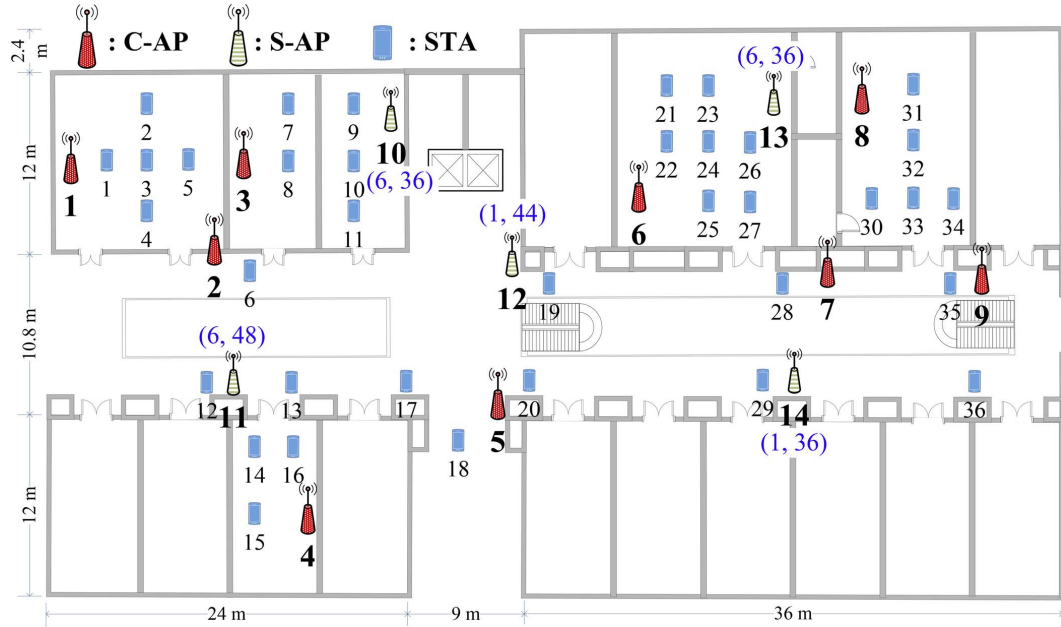
Fig. 4.1: Experimental indoor environment.

Another channels having bandwidth wider than a basic channel can be constructed by bonding multiple non-overlapped basic channels. Then, there are a total of five channels in the 2.4 GHz band: four basic channels and one bonding channel of 40 MHz. In addition, there are a total of seven channels in the 5 GHz band: four basic channels, two 40 MHz bonding channels, and one 80 MHz bonding channel. Each S-AP only uses a single basic channel, whereas a C-AP can use not only a basic channel but also a bonding channel. As seen in Fig. 4.1, the channels assigned to each S-AP is expressed as a pair of channel numbers in each band with blue numbers around corresponding S-AP, such as (2.4 GHz-channel, 5 GHz-channel). The total number of STAs in the network is denoted by N and the maximum value of N in our experiment is 36. When the STAs are deployed at maximum, the position of each STA (from STA-1 to STA-36) is like in Fig. 4.1.

4.1.3 Experimental Setting

We conduct the experiments, gradually increasing N by 6, i.e., N is changed to $6, 12, \cdots, 30, 36$. When increasing N by one level, we select six STAs with index difference of 6, in sequence, so that the selected STAa can be more evenly distributed in the network. As an example, suppose that the index set of existing six STAs is $\{2, 8, 14, 20, 26, 32\}$. Then, the index set of 12 STAs including newly added 6 STAs may be $\{2, 4, 8, 10, 14, 16, 20, 22, 26, 28, 32, 34\}$.

In order to measure the throughput per STA, the UDP traffic is generated at the rate of α by using *iperf* and is transmitted to each STA associated with S-AP or C-AP. To avoid the interference from other external APs in the building, experiments are conducted for the time with little external traffic (e.g., late night or early in the morning). In the CA scheme, the RSSI thresholds for generating the interference graph are $\xi_{\text{CCA-CS}} = -82$ dBm, $\xi_{\text{CCA-ED}} = -62$ dBm. The parameter values for the proposed UA scheme are $T_{\text{UA}} = 5$ min and $L_{\text{th}} = 0.9$.

The performance metrics are as follows: average throughput per STA, total throughput of STAs in the network, and fairness. The Jain's fairness index is adopted as fairness metric: $\psi = \left(\sum_{i=1}^{N} \Phi_i \right)^2 / \left(N \cdot \sum_{i=1}^{N} \Phi_i{}^2 \right)$, where Φ_i is the throughput of STA-i. Note that $\frac{1}{N} \leq \psi \leq 1$. When ψ is close to 1, all STAs are expected to get almost the same throughput.

4.1.4 Comparison Schemes

For performance comparison with the proposed RRM, we implemented some RRM schemes, which combine existing CA and UA schemes. As the existing CA schemes for comparison, we took the random channel selection (RCS) scheme and the cen-

tralized version of CA scheme in [3] (namely, LIC). In the RCS, a basic channel or a bonding channel is randomly allocated to each C-AP. In the LIC, the controller assigns a basic channel with the least number of interference sources to each AP, based on the interference graph.

As the existing UA schemes for comparison, we choose RSSI-based UA, band-steering in [18] (namely, BSTR), and FAME in [10]. The RSSI-based UA selects the AP/band with the highest RSSI among neighboring APs. The BSTR scheme in [18] coordinates the ratio between the number of STAs in 2.4 GHz band and that in 5 GHz band, where each STA firstly selects the C-AP with the highest RSSI as its serving AP and then each C-AP performs the ratio coordination. The FAME scheme in [10] makes a connection between AP/band and each STA for maximizing the MAC efficiency metric, which is derived based on the link rate, traffic amount, and collision rate.

4.1.5 Experimental Results

Table 4.1 shows the CA results for C-APs in each comparison scheme. Since the RCS scheme randomly allocates channels to C-APs, neighboring APs can use the same or overlapped channels. For example, the AP-1, AP-2, and AP-3 being adjacent to each other use overlapped channels in the 2.4 GHz band and, the AP-1 and AP-3 use the same channel in the 5 GHz band. We can predict severe interference among these APs in both bands. The LIC scheme allocates a basic channel to each C-AP while reducing the interference among neighboring APs. As compared with the RCS scheme, neighboring APs use different channels to minimize the CCI in the 5 GHz band, but there still exists the ACI in the 2.4 GHz band due to the deficiency of non-overlapped channels. In our proposed CA

Tab. 4.1: Channel assignment results (2.4 GHz ch., 5 GHz ch.).

	RCS	LIC	Proposed
AP-1	(4, 48)	(1, 40)	(1, 36-40)
AP-2	(2, 36)	(6, 36)	(6, 48)
AP-3	(1, 44-48)	(4, 44)	(6, 44)
AP-4	(6, 44)	(2, 48)	(1, 36-40)
AP-5	(1, 40)	(2, 48)	(1, 48)
AP-6	(4, 36-40)	(6, 44)	(6, 40)
AP-7	(6, 48)	(4, 40)	(2, 40)
AP-8	(2, 40)	(1, 48)	(6, 44-48)
AP-9	(2, 36)	(2, 36)	(2, 36)

scheme, channels are allocated to C-APs under consideration of mutual interference among APs (S-APs and C-APs). In particular, bonding channels can be allocated to some APs (AP-1, AP-4, and AP-8) in the 5 GHz band while minimizing the mutual interference. For this reason, the network performance of the proposed CA scheme would be better than that of LIC.

Tab. 4.2: Performance comparison ($N = 36$, $\alpha = 15$ Mbps).

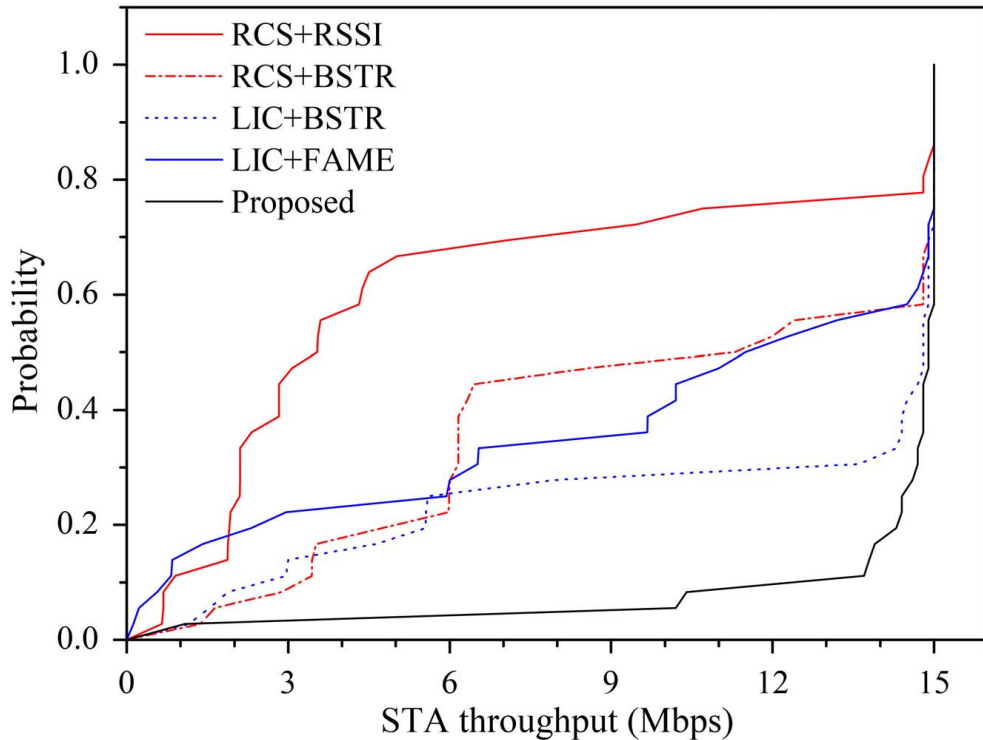|	RCS+ RSSI	RCS+ BSTR	LIC+ FAME	LIC+ BSTR	Proposed
Average STA throughput (Mbps)	6.21	9.99	7.14	11.79	14.14
Fairness	0.56	0.80	0.77	0.85	0.97

Fig. 4.2: CDF of STA throughput ($N = 36$, $\alpha = 15$ Mbps).

Fig. 4.2 shows the cumulative distribution function (CDF) of STA throughput, when the number of STAs within the network, N, is 36 and the traffic generation rate of a STA, α, is 15 Mbps. Also, Table 4.2 presents the average STA throughput and fairness in the same settings.

Firstly, we compare the performance of CA schemes from Fig. 4.2 and Table 4.2. Under the RCS scheme assigning the channels randomly, there exists severe inter-ference (CCI and/or ACI) among APs because neighboring APs may use the same or adjacent channels. Whereas, in the LIC scheme, neighboring APs use different channels to minimize the CCI in the 5 GHz band. This results in the performance

gap between RCS and LIC, which can be observed by comparing two cases of using BSTR scheme in Fig. 4.2 and Table 4.2. In our proposed CA scheme [9], an available channel (basic channel or bonding channel) is allocated to each C-AP under consideration of direct/hidden interference. Since STAs associated with those C-APs suffer from the relatively less interference, the throughput performance of the STAs is enhanced.

Next, let us discuss the performance of UA schemes from Fig. 4.2 and Table 4.2. Note that the STAs associated with the channels of 2.4 GHz band are more severely influenced by the interference among APs, compared with the STAs in 5 GHz band. [1] Thus, with the same CA scheme randomly selecting the channels (i.e., RCS), the RSSI-based UA provides much lower performance than the BSTR-based UA, where some STAs in the 2.4 GHz band can be moved to the 5 GHz band for load balancing after initial UA based on RSSI. On the other hand, the performance of the FAME UA scheme in [10] is much lower than that of BSTR scheme. This is because the FAME scheme does not consider the interference factor, even if a considerable number of STAs are associated with APs in the 2.4 GHz band having the severe interference. Furthermore, some STAs can be associated with APs of which RSSI is relatively low because the UA between AP/band and each STA is determined based on only the MAC efficiency defined in [10]. Then, the throughput performance of these STAs, particularly in the 2.4 GHz, can be very

---

[1]Generally, frequency characteristic (*e.g.,* diffraction, penetration) of 2.4 GHz band is even better than that of 5 GHz band. However, such characteristic in the dense WLAN environment unfortunately has harmful effects on interference. Furthermore, in the 2.4 GHz band, there are overlapped channels causing the ACI. For this reason, the interference level is much higher in the 2.4 GHz band than in 5 GHz band.

Tab. 4.3: Performance comparison ($N = 36$, $\alpha = 25$ Mbps).

	RCS+ RSSI	RCS+ BSTR	LIC+ FAME	LIC+ BSTR	Proposed
Average STA throughput (Mbps)	8.44	13.57	9.29	15.73	19.97
Fairness	0.46	0.68	0.68	0.74	0.93

low. As a result, about 30% of total STAs have the throughput less than 6.5 Mbps, and the average STA throughput is merely 7.14 Mbps. Owing to the performance gap between STAs in the two frequency bands, the fairness becomes relatively low as 0.77 (see Fig. 4.2 and Table 4.2). However, note that although BSTR is used, there are still a considerable number of STAs in the 2.4 GHz band and these STAs suffer from performance degradation due to the interference among APs.

In contrast, by using the proposed UA scheme, STAs can be associated with non-overlapped channels of each band in a balanced way. In addition, since only STAs which can be accommodated to each channel of S-APs and C-APs under consideration of both channel interference and traffic amount are associated with the APs, the utilization ratio of the total frequency resource is significantly enhanced. For this reason, as seen in Fig. 4.2, the overall throughput performance of STAs in the proposed scheme is much higher than in the comparison schemes. Also, since there exists the very small performance gap among STAs, the fairness value is close to 1, as shown in Table 4.2.

Fig. 4.3 depicts the CDF of STA throughput when $N = 36$ and $\alpha = 25$ Mbps, and Table 4.3 shows the average STA throughput and fairness in the same settings. Although α increases to 25 Mbps, the performance trend is very similar with the
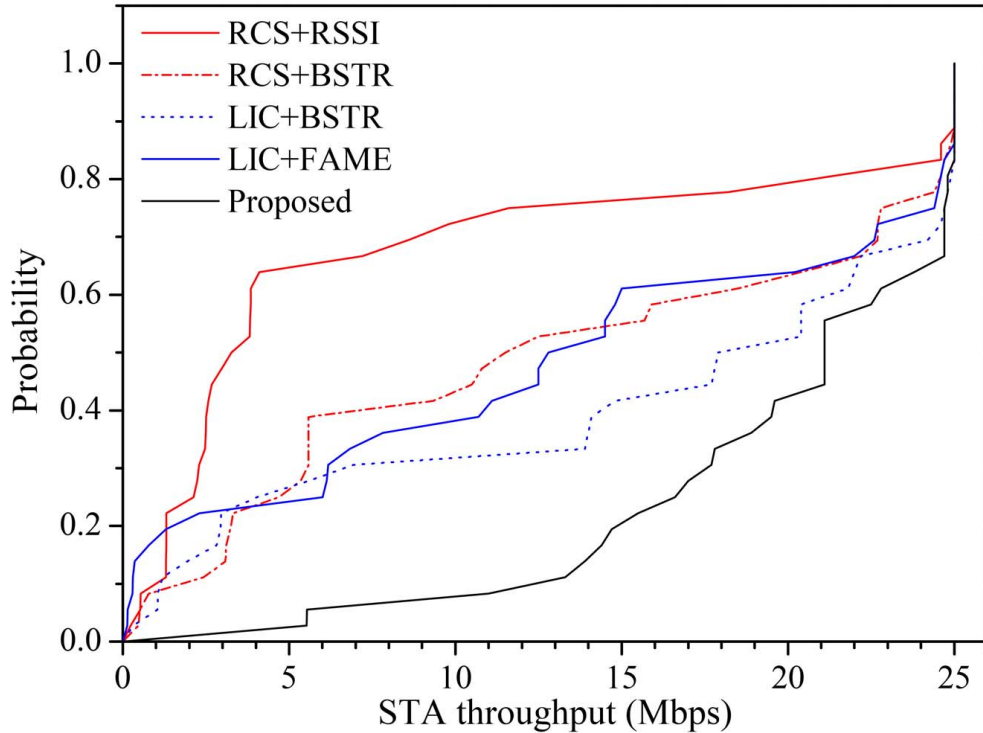
Fig. 4.3: CDF of STA throughput ($N = 36$, $\alpha = 25$ Mbps).

results when $\alpha = 15$ Mbps in Fig. 4.3 and Table 4.3. Owing to larger performance gap between STAs in each band, the fairness value is less with $\alpha = 25$ Mbps than $\alpha = 15$ Mbps, in all schemes. However, the decrease of fairness in the proposed scheme is much smaller than that in the other schemes.

Table 4.5 shows the performance comparison between the two frequency bands, where $N = 36$ and $\alpha = 25$ Mbps. Under the proposed scheme in comparison with the other schemes, even if there are much more STAs associated to 5 GHz band, the average STA throughput in 5 GHz band is maintained to a relatively high value above 20 Mbps. Moreover, the performance gap between the two frequency

Tab. 4.4: Comparison between two frequency bands ($N = 36$, $\alpha = 25$ Mbps).

	Band (GHz)	Number of STAs	Avg. STA Throughput (Mbps)	Total Throughput (Mbps)
RCS+RSSI	2.4	31	5.88	182.49
	5	5	24.28	121.4
RCS+BSTR	2.4	19	14.06	267.10
	5	17	13.02	221.36
LIC+FAME	2.4	18	8.25	148.49
	5	18	19.12	344.19
LIC+BSTR	2.4	20	11.16	223.14
	5	16	21.46	343.3
Proposed	2.4	10	18.44	184.4
	5	26	20.56	534.57

bands in the average STA throughput is very small. For this reason, as depicted in Table 4.3, the average STA throughput and fairness are much higher than those of comparison schemes.

Fig. 4.4 and Fig. 4.5 show the total throughput and fairness according to N, respectively, when $\alpha = 15$ Mbps. In the RSSI-based UA combined with RCS CA, even if N is larger than 18, the total throughput is maintained without greatly increasing. This is because there are a relatively large number of associated STAs in the 2.4 GHz band having low capacity. As shown in Fig. 4.4, the enhancement ratio of the total throughput according to increasing N is higher in the proposed scheme than in comparison schemes. Accordingly, the performance gaps in total
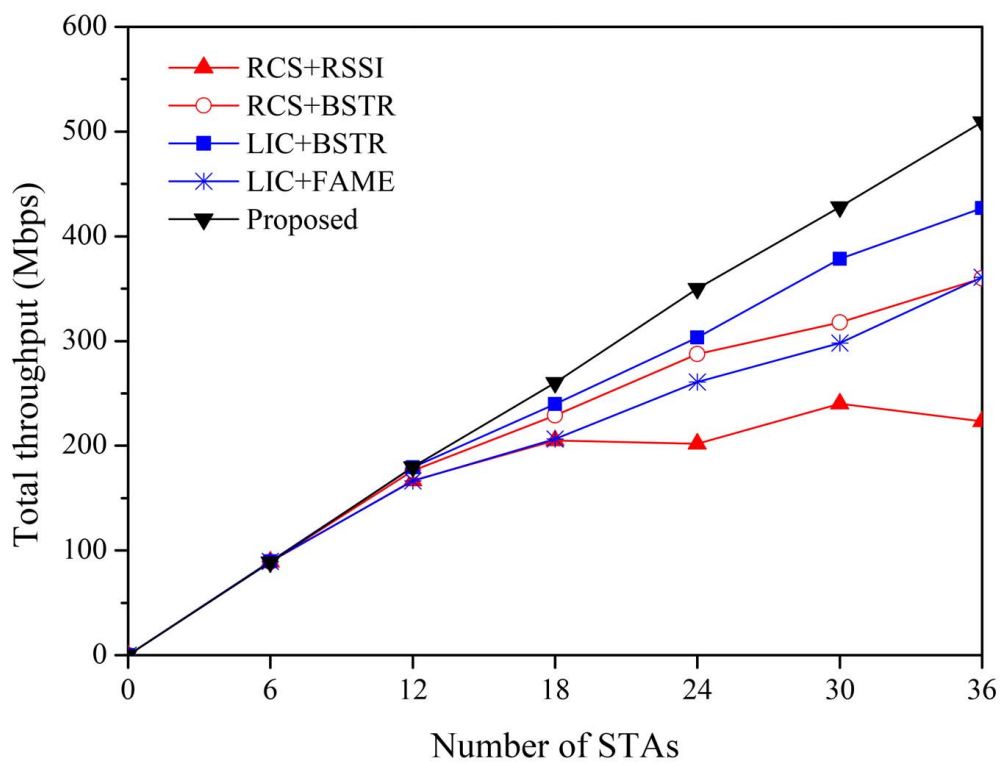
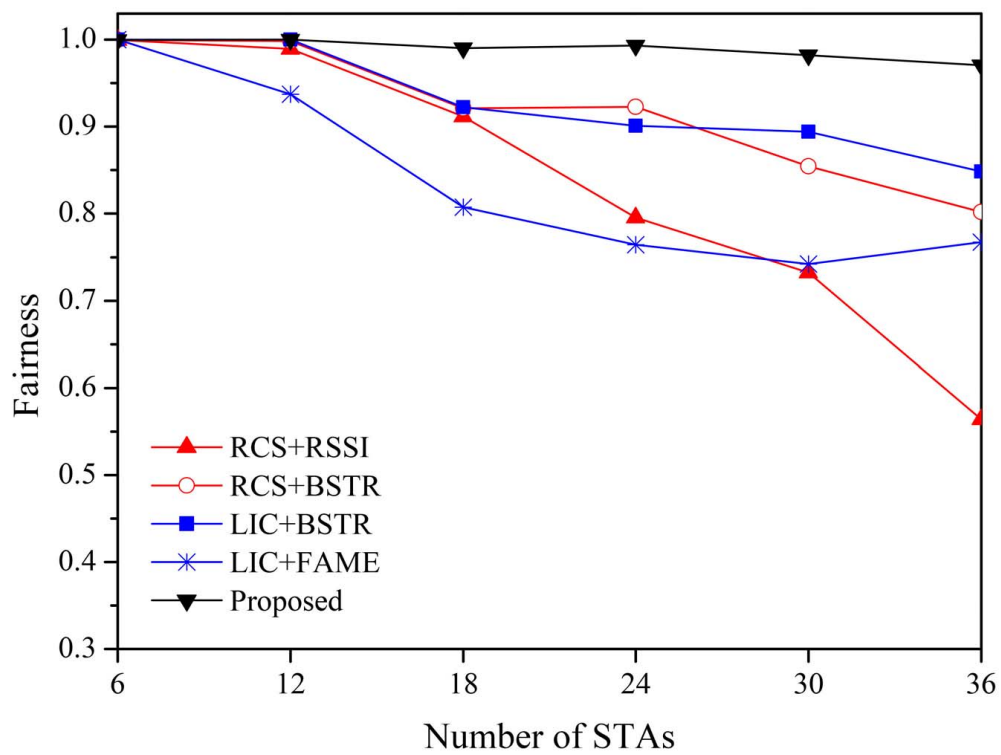Fig. 4.4: Total throughput according to N ($\alpha = 15$ Mbps).

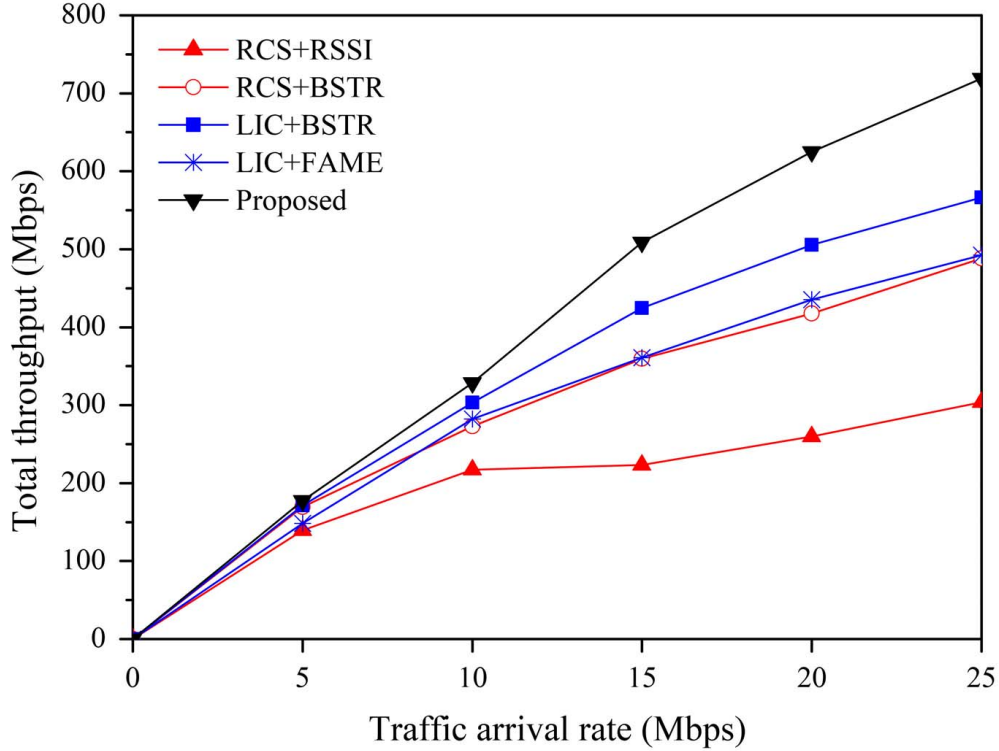Fig. 4.5: Fairness according to N ($\alpha = 15$ Mbps).

Fig. 4.6: Total throughput according to α ($N = 36$).

throughput between the proposed and other schemes get larger as N increases. On the other hand, we can see in Fig. 4.5 that, under the comparison UA schemes (i.e., RSSI-based, BSTR, and FAME), the fairness greatly decreases with the increases of N. This is because the number of STAs associated with 2.4 GHz band (as a result, the number of STAs having low throughput) increases. On the contrary, in the proposed RRM, the total throughput linearly increases with increasing N (see Fig. 4.4). Furthermore, as shown in Fig. 4.5, the fairness value is close to 1, since most of STAs in the network maintain the high throughput and the performance gap among the STAs is very small.

Fig. 4.6 and Fig. 4.7 depict the total throughput and fairness according to α, respectively. As seen in Fig. 4.6, when α increases, the total throughput increases but its enhancement ratio gradually decreases. Especially, in the RCS CA and RSSI-based UA scheme, when $\alpha \geq 10$ Mbps, the total throughput becomes saturated. With increasing α, the performance gaps in total throughput and fairness between the proposed RRM and other schemes get larger. In the comparison schemes, the fairness value is significantly decreased with increasing α. On the contrary, in the proposed RRM, when α increases, the fairness value is maintained close to 1 (see Fig. 4.7). This means that the proposed CA method effectively allocates channels so that the interference among APs is minimized. Furthermore, by the proposed UA-ChLB scheme, the frequency resource of S-APs and C-APs is efficiently utilized under consideration of several factors such as wireless channel quality, traffic amount, and channel interference level.
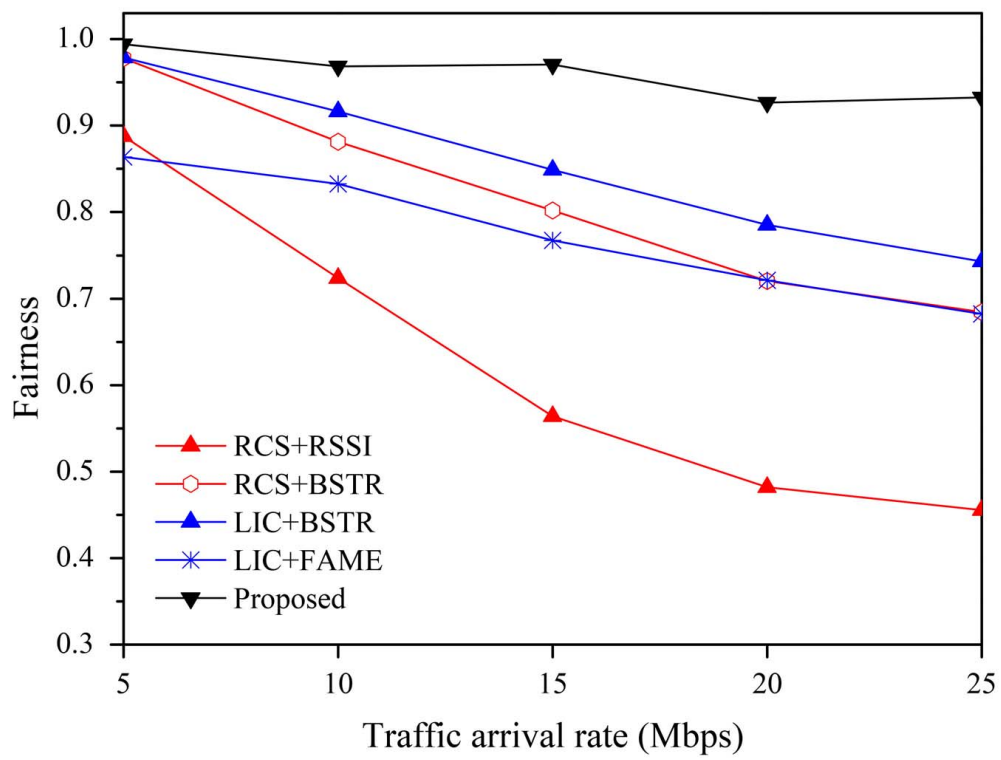
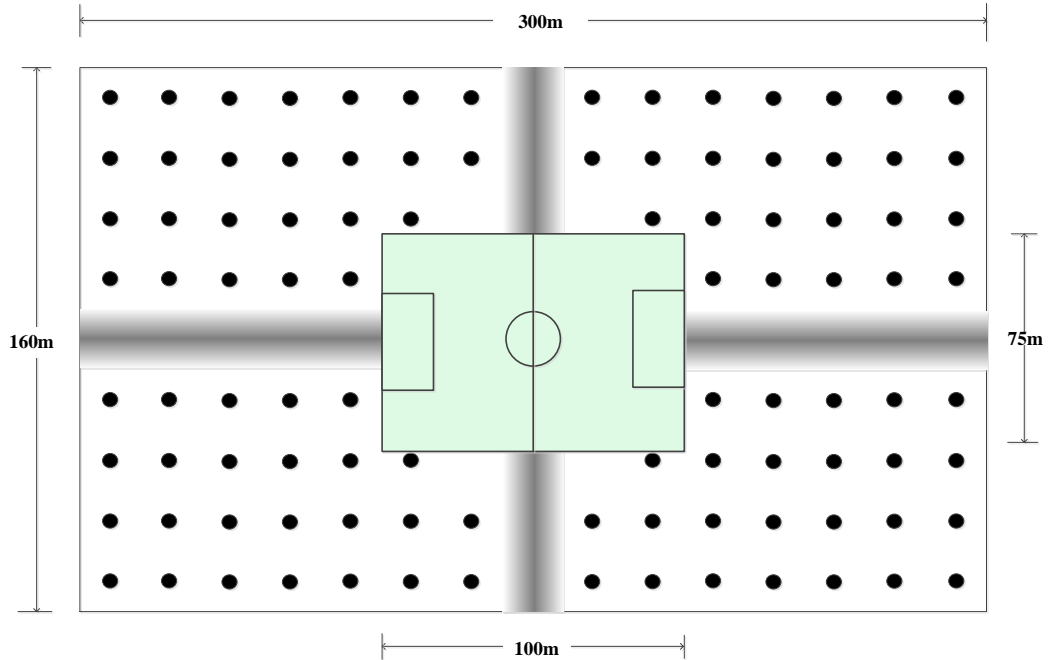Fig. 4.7: Fairness according to α ($N = 36$).

Fig. 4.8: Simulation environment of soccer stadium.

4.1.6 Simulation Environment

To evaluate performances of proposed RRM and comparison schemes in the ultra dense WLAN environment, ns-3 network simulator can be utilized. However, the ACI factor was not considered in the ordinary implementation of ns-3. To tackle this issue, authors in [28] implemented a WiFi ACI model by introducing the function *overlapFactorToBeDecoded* which calculates the leakage power ratio causing the ACI and modified several WiFi modules of ordinary ns-3 (version 3.26) in the file of *yans-wifi-channel.cc*. According to the validations in [28] based on simulations and actual experiments on the testbed, the ACI factor is well applied in the modified part of ns-3. The detailed explanations of the modification in the ns-3 and its validations are described in [28]. Therefore, we have utilized the modified

60

source codes of ns-3 in [29] and have conducted extensive simulations.

Fig. 4.8 shows the soccer stadium environment, where a total of 100 APs using IEEE 802.11n/ac are deployed. Let us assume that there exist 1000 STAs that associated to the APs among whole spectators for the purpose of data offloading. The transmission power of each AP is set to 10 dBm. In the 2.4 GHz band, APs use 13 basic channels from ch. 1 to 13. In the 5 GHz band, APs use 9 basic channels (ch. 36, 40, 44, 48, 149, 153, 157, 161, 165), and four 40 MHz channels (ch. 38, 46, 151, 159), and two 80 MHz channels (ch. 42, 155).

4.1.7 Simulation Setting

Under consideration of stadium environment, we assume that all of deployed APs are C-APs connected to a controller, and there is no external traffic in the stadium. As a propagation model in ns-3, the log-distance pathloss model is used. To measure the throughput per STA, the constant UDP traffic is generated at the rate of α and is transmitted to each STA associated with the AP. In the CA scheme, the RSSI thresholds for generating the interference graph are $\xi_{\text{CCA-CS}} = -82$ dBm, $\xi_{\text{CCA-ED}} = -62$ dBm. For the UA scheme, only the distributed UA methods are conducted to reduce the computational complexity under consideration of a large number of STAs in the stadium environment. The parameter value for the proposed UA scheme is $L_{\text{th}} = 0.9$. The performance metrics are the total throughput of STAs and fairness. The comparison schemes are same with the RRM schemes used in the experimental results as follows. As the CA schemes, the random channel selection (RCS) scheme and the centralized version of CA scheme in [3] (namely, LIC) are used. As the UA schemes, RSSI-based UA, band-steering in [18] (namely, BSTR), and FAME in [10] are used.

61

Tab. 4.5: Performance comparison ($N = 1000$, $\alpha = 2.5$ Mbps).

	RCS+ RSSI	RCS+ BSTR	LIC+ FAME	LIC+ BSTR	Proposed
Average STA throughput (Mbps)	1.01	1.49	1.51	1.57	1.81
Fairness	0.53	0.71	0.74	0.77	0.88

4.1.8 Simulation Results

Compared with the experimental indoor environment, there are a considerable number of APs and STAs in the soccer stadium environment of Fig. 4.8. For this reason, it is expected that the interference among APs becomes severe and the STA throughput gets lower.

Table 4.5 depicts the average STA throughput and fairness, where $N = 1000$ and $\alpha = 2.5$ Mbps. Since the RCS scheme randomly allocates channels, there exists severe CCI and ACI among neighboring APs. Furthermore, through the RSSI-based UA, the channel load and interference in 2.4 GHz band gets higher. For this reason, the average STA throughput and fairness are very low. However, even if the RCS scheme is used, the performance can be greatly increased by merely utilizing the BSTR UA. This means that reducing the interference in the $2.4GHz$ is considerably effective. Also, when the BSTR or FAME UA is used, the performance can be enhanced a little by using the LIC CA scheme. This is because there is still the severe ACI in the densely deployed environment.

On the other hand, for such environment, the CCI/ACI among APs can be efficiently coordinated by using the proposed CA. Also, each STA can select AP/band
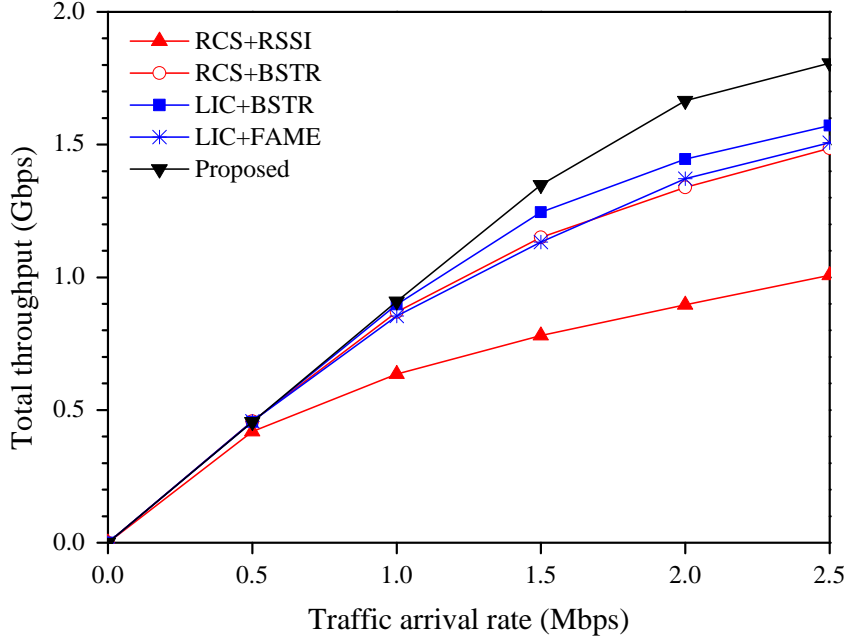
Fig. 4.9: Total throughput according to α ($N = 36$).

having the low channel load by the proposed UA-ChLB in a distributed manner. Therefore, the average STA throughput and fairness values of the proposed scheme are far higher than those of other schemes.

Fig. 4.9 and Fig. 4.10 show the total throughput and fairness according to α, respectively. As shown in Fig. 4.9, when α increases, the total throughput increases but its enhancement ratio gradually decreases due to the capacity limitation. With increasing α, the performance gaps in total throughput and fairness between the proposed RRM and other schemes become larger. As shown in Fig. 4.10, the fairness value becomes smaller with increasing α, but its decreasing ratio of the proposed RRM is much smaller than that of comparison schemes. Especially, in
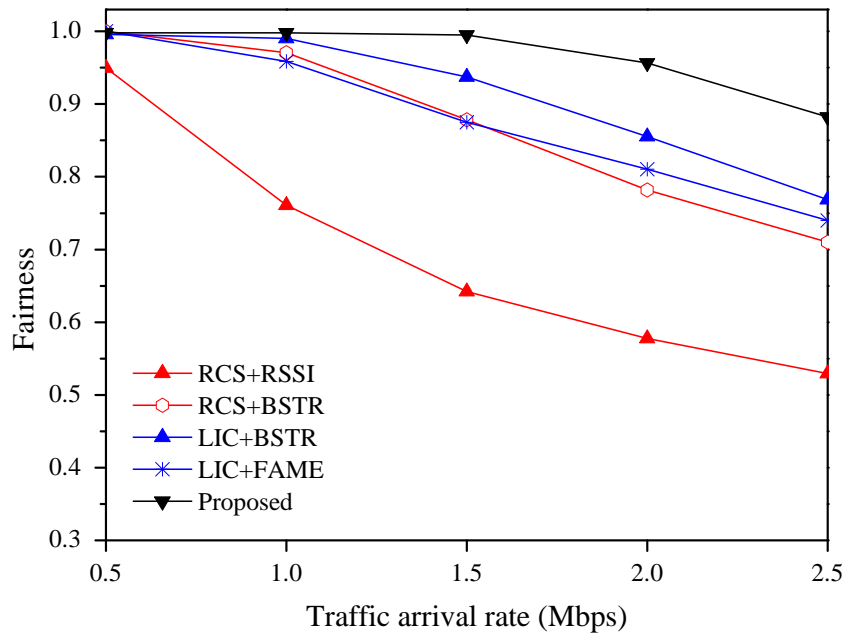
Fig. 4.10: Fairness according to α ($N = 36$).

the proposed RRM, when $\alpha \leq 2.0$, the fairness value is maintained close to 0.95. Therefore, through the simulation results compared with other schemes, we can observe that the proposed CA method effectively assigns channels and the proposed UA-ChLB scheme effectively utilizes the frequency resource of APs in the extremely dense WLAN environment.

4.2 MDP-based Block Length Decision Method

4.2.1 Simulation Setting

We refer to the IEEE 802.15.4z standard in setting the values of simulation parameters. In the standard, the slot length, L_{slot}, is 1200 RSTUs and the length of a ranging round, L_{round}, is 20 L_{slot}. Since an RSTU is 833.33 ns, $L_{\text{slot}} = 0.001$ s and $L_{\text{round}} = 0.02$ s, respectively. The arrival rate of update requests is set to the same rate λ for all RDEVs under consideration of the expected number of requests during an active round. In simulation, we set the preferred block length of an RDEV to a different value from each other, as follows: the RDEV-n has the preferred block length such that $g(n) = 2n \ L_{\text{round}}$. Thus, when N is the number of RDEVs, $\mathcal{L} = \{2L_{\text{round}}, 4L_{\text{round}}, \cdots, 2NL_{\text{round}}\}$. Also, $L_{\text{bmin}} = 2L_{\text{round}}$ and $L_{\text{bmax}} = 2NL_{\text{round}}$. The discount factor β is set to 0.9. We obtain the performance measures for each parameter by averaging the results from 300 simulation runs, where the total ranging time of each simulation run is 600 s.

As metrics for performance evaluation, we adopt a ranging frequency and an average request acceptance ratio. The ranging frequency is defined as the average number of ranging blocks per second. Since there is one active round within a ranging block and the RDEVs conduct the ranging operation during the active round, the ranging frequency actually corresponds to the total number of active rounds for a second. Since the RDEVs keep awake only during the active rounds and each round has a fixed time-length, the RDEVs consume more energy with more active rounds for a second, i.e., with the higher ranging frequency. Thus, the ranging frequency is a metric for assessing the energy consumption. Considering that IoT devices should survive for a long time with a small battery capacity, the

ranging frequency can be especially an important metric.

The average request acceptance ratio of the ranging group is another metric for assessing the satisfaction level of each RDEV. This metric is obtained by averaging the request acceptance ratios of RDEVs, where the request acceptance ratio of each RDEV is calculated as the proportion of the accepted requests among all transmitted requests of the RDEV for a simulation run. Naturally, when there are multiple RDEVs that send requests in a ranging group, the average request acceptance ratio becomes less than 1.0. Also, when the number of RDEVs in the ranging group or the number of transmitted requests increases, the ratio gets low.

Since there is no existing works of the request-based dynamic block length decision for IEEE 802.15.4z, we have additionally designed simple but efficient baseline schemes for the comparisons. In the longest waiting selection, the controller selects the request being not accepted during the most blocks. When there are two or more candidates, one is randomly selected. The highest satisfaction selection scheme chooses the request which maximizes $\sum_{n=1}^{N} \left(1 - \frac{x_n \cdot |\ell_i - g(n)|}{L_{\mathrm{bmax}} - L_{\mathrm{bmin}}} \right)$ by utilizing a satisfaction function of a linear form defined in (3.5). If there are two or more candidates, this scheme also randomly selects one. The median selection means selecting the request whose preferred length is the median of the preferred lengths of the requests. When the number of the requests is even, there are two candidates for median. Then, the request with the smaller preferred length is accepted.

4.2.2 Simulation Results

Fig. 4.11 shows the ranging frequency and the average request acceptance ratio according to the reward function type and w which is the relative weight of energy saving to satisfaction, when $N = 8$ and $\lambda = 0.3$. As w increases, the controller
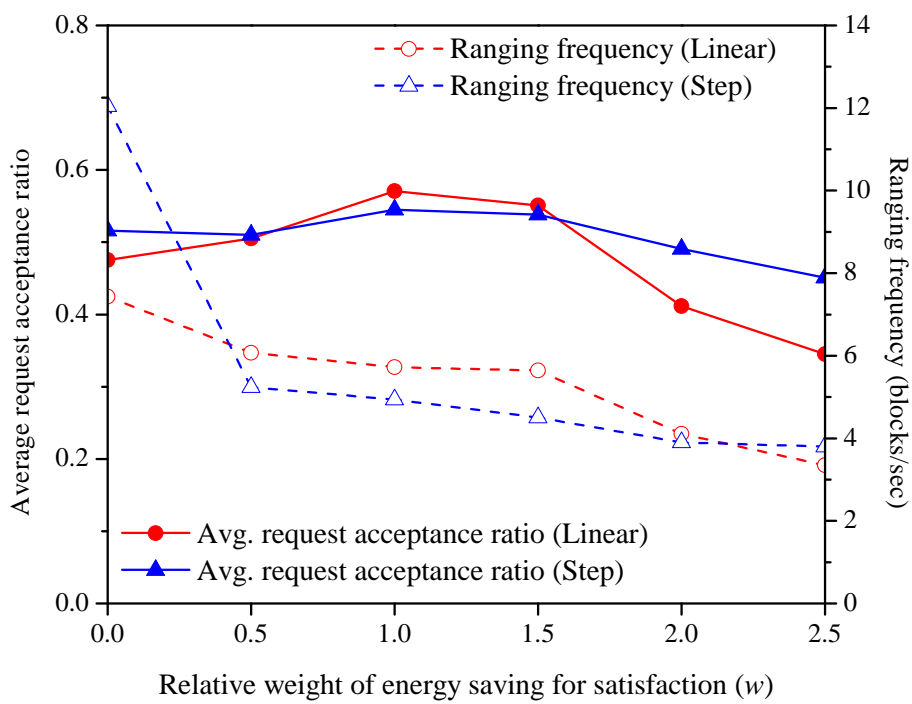
67

Fig. 4.11: Performance of the proposed scheme according to w ($N = 8$, $\lambda = 0.3$).

considers the energy saving as being more and more important, in deciding the block length. Thus, with the larger w, the block length gets longer and this leads to the lower ranging frequency. When w increases, in both linear and step functions, the average request acceptance ratio has a concave shape (i.e., increases and again decreases). With too small w such as $0 \le w \le 0.5$, since the controller concentrates on obtaining a high satisfaction reward, it mainly chooses the request whose length is close to the median of requested lengths. This incurs a big difference between the request acceptance ratios of the RDEVs and lowers the average request acceptance ratio of the group. As w increases, this situation is relieved and the average request acceptance ratio also increases. However, as examined in the discussion on the ranging frequency according to w, a large w results in a long ranging interval and this incurs more requests during one active round. Thus, if w continues to increase (e.g., $w \ge 1.5$), as shown in the figure, the average request acceptance ratio does not increase but rather decreases. In general, it is apparent that the lower ranging frequency (lower energy consumption) and the higher request acceptance ratio are more desirable. Based on Fig. 4.11, in both cases, it is probably recommendable that $0.5 \le w \le 1.5$ for the given parameter setting.

Figs. 4.12 and Figs. 4.13 depict the performance of the proposed scheme according to the update request generation rate of an RDEV, λ, when $N = 8$. An increase of λ means more requests within a ranging block and this obviously incurs the lower acceptance ratio. Furthermore, since each RDEV has a different preferred block length, the average of the preferred block lengths of the requests within a ranging block increases with more requests. That is, the required average block length increases. Thus, the ranging frequency decreases as λ increases. On the other hand, the figure also shows the effect of w on the performance of the
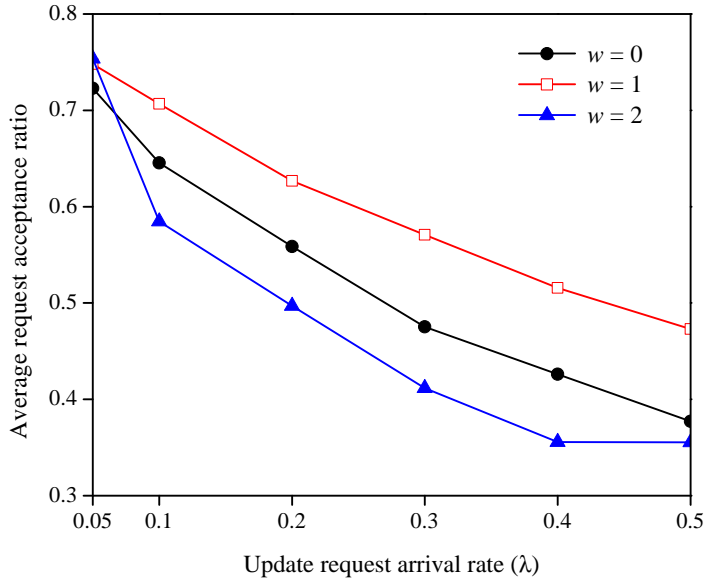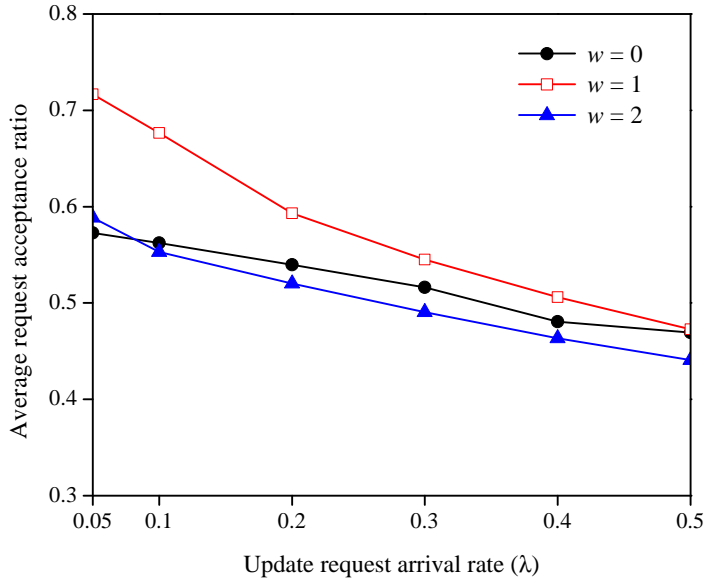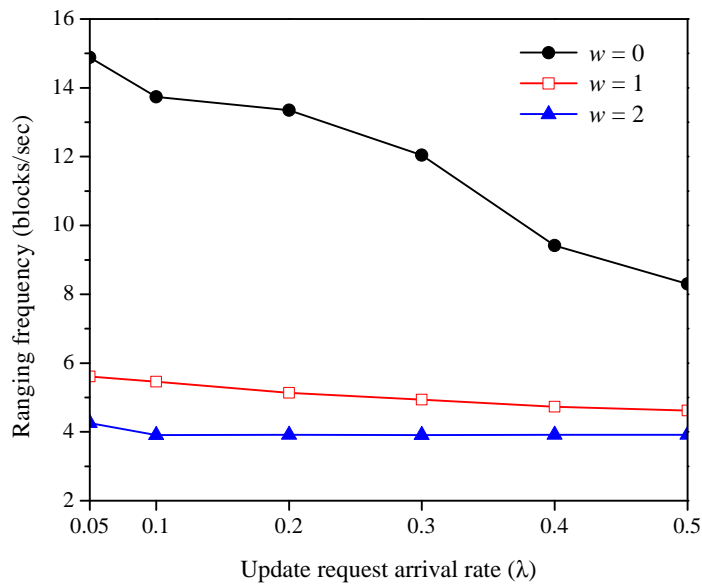
(a) Average request acceptance ratio
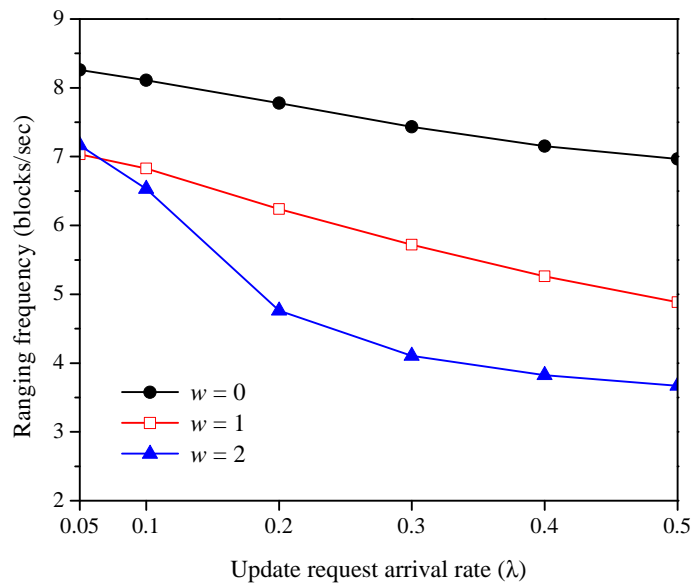
(b) Ranging frequency

Fig. 4.12: Performance of the proposed scheme according to λ ($N = 8$, Linear).

(a) Average request acceptance ratio

(b) Ranging frequency

Fig. 4.13: Performance of the proposed scheme according to λ ($N = 8$, Step).

proposed scheme. As already observed in Fig. 4.11, in pursuing the lower ranging frequency and the higher average acceptance ratio together, it is better to consider these two factors with similar importance, i.e., $w = 1$.

Fig. 4.14 presents the performance comparison between the proposed scheme (linear, step) and three baseline schemes according to λ, when $N = 8$ and $w = 1$. With a larger λ, since each RDEV generates more frequently a request, the number of the requests at each active round increases. From the view point of the ranging group, only a single request can be accepted in the decision epoch among several requests received from multiple RDEVs. Therefore, in all of four schemes, it is natural that the average request acceptance ratio decreases for the increased λ. Even if λ is low, the average request acceptance ratio is less than 1.0. Also, as already discussed in Fig. 4.13, the average of the preferred block lengths of the requests within an active round increases with more requests. Accordingly, the ranging frequency decreases with a larger λ, irrespective of the schemes.

Next, we compare the performances of four schemes according to λ, in Fig. 4.14. The longest waiting selection scheme carries out a kind of the first-in first-out (FIFO) selection without considering the preferred lengths of requests. Thus, a request under this scheme should be repetitively retransmitted during much more blocks until it is accepted, as compared with the other schemes. Accordingly, the longest waiting selection scheme has the lowest average request acceptance ratio [see Fig. 4.14(a)]. On the other hand, since the highest satisfaction selection scheme chooses the request maximizing the satisfaction reward among the requests, it achieves a good performance in the average request acceptance ratio. However, since the energy saving is not considered in deciding the block length, this scheme performs the ranging operation more frequently with the shorter interval, i.e., it has

the highest ranging frequency among the schemes [see Fig. 4.14(b)]. The median selection scheme achieves a properly good performance, by selecting the request having the median preferred length among the received requests. But, it makes a static decision based on only the requests within the same active round without the consideration of the performance metrics, whereas the proposed scheme (linear, step) prefers the shorter block length for energy saving while reducing the difference between the selected block length and the requested block lengths. That is, the proposed scheme (linear, step) adaptively determines the block length for maximizing the expected future reward directly related to the performance metrics. As a result, the proposed scheme (linear) provides the best performance in energy saving while reasonably preserving the high average request acceptance ratio, in comparison of all other schemes. Furthermore, the proposed scheme (step) can greatly enhance while slightly reducing the average request acceptance ratio.

Fig. 4.15 shows the performance comparison results according to the number of RDEVs, when $\lambda = 0.3$ and $w = 1$. In all of four schemes, it is observed that a larger N leads to the smaller acceptance ratio and the lower ranging frequency. The reason is as follows. As the number of RDEVs increases, since more requests are transmitted for each active round, it is natural that the average request acceptance ratio decreases. Remind that, in our simulation model, the preferred block length of RDEV-n is set to $2nL_{\text{round}}$. Accordingly, whenever N increases by one, since an RDEV with the longer preferred block length is added, the average preferred block length within a ranging group increases and this results in the longer block. Thus, the ranging frequency gets lower with a larger N. On the other hand, we can observe that the performance comparison result among the schemes for the increase of N in Fig. 4.15 demonstrates a similar tendency with the performance

73

comparison result according to λ in Fig. 4.14. This is because the increase of N has a similar effect with the increase of λ. That is, like when the update request generation rate of an RDEV, λ, is increased, more requests at each active round are transmitted with more RDEVs within a group. As shown in Fig. 4.15, the proposed scheme (linear, step) still outperforms other comparison schemes in all of two performance metrics.

4.2.3 Implementation Capabilities

Some recently released mobile devices, such as Apple iPhone 11/12, Samsung Galaxy Note 20, are equipped with UWB chipset to provide highly accurate UWB-based ranging/localization services, but these devices merely support own ranging/localization service applications provided by their vendors. To the best of our knowledge, these service applications cannot be modified and general developers cannot access or control UWB operations in these devices yet.

On the other hand, to realize the proposed scheme on these commercial devices, there should be the proper UWB API to access or control UWB operations in the devices as follows. First, a function for sending an RPUM which contains a preferred block length of each RDEV should be included in the UWB API. In the in-band signaling manner of IEEE 802.15.4z standard, each responder can send the RPUM with its response or report message (RM and MR of active round) together and the initiator can send its RPUM during the RIP or RFP of the active round. Second, to adapt the ranging block length that is determined based on the received requests, a function for setting the ranging block length by a controller RDEV should be included in the UWB API. Through these two functions, the proposed scheme can be implemented in the real devices.

Fortunately, Google has currently been developing an official UWB API complying with IEEE 802.15.4z for Android devices [48], so that Android version 12 including the UWB API will be released in the first half of 2021. It is expected that those necessary functions would be included in the official UWB API. Therefore, the proposed time resource management method can be implemented on them in the near future.
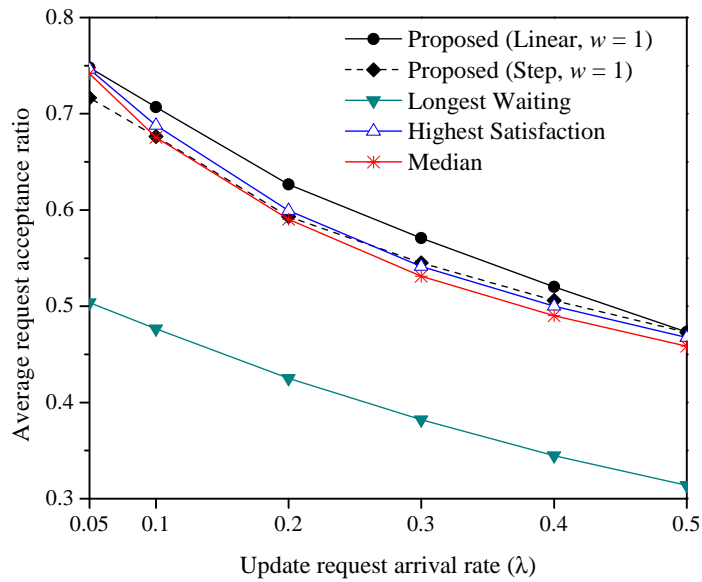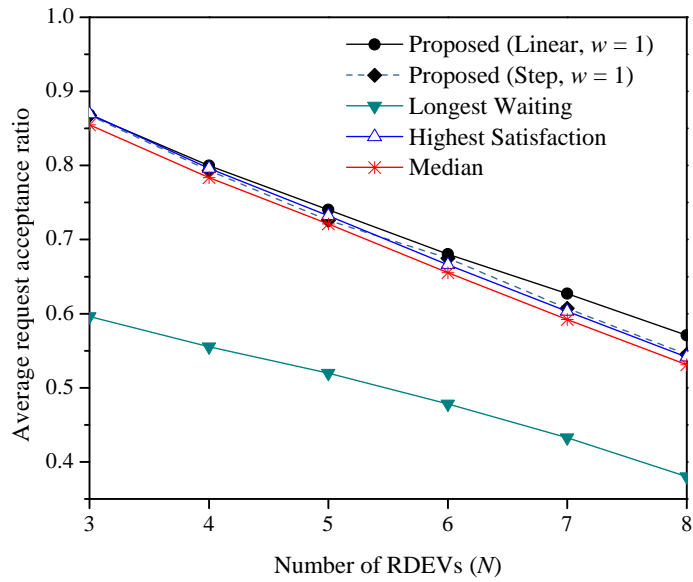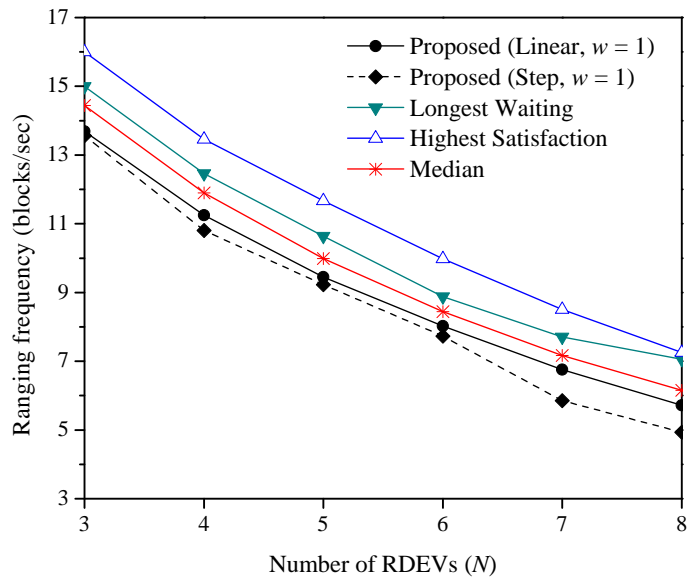
(a) Average request acceptance ratio
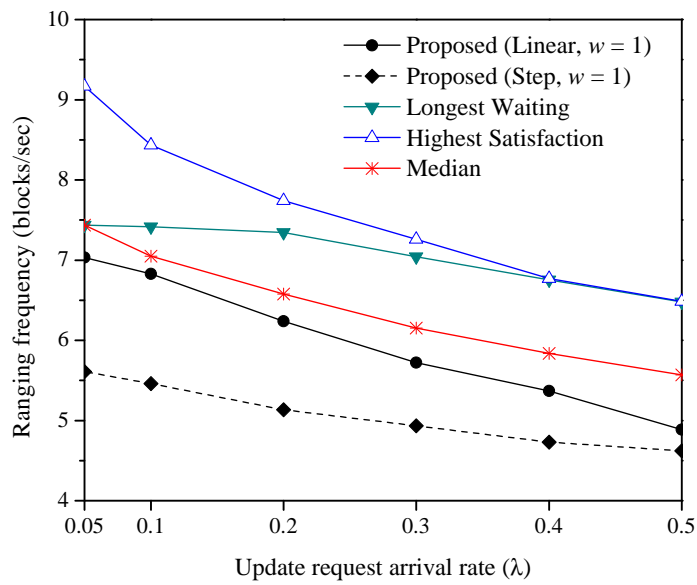
(b) Ranging frequency

Fig. 4.14: Performance comparison between the proposed scheme and three baseline schemes according to λ ($N = 8$, $w = 1$).

(a) Average request acceptance ratio

(b) Ranging frequency

Fig. 4.15: Performance comparison between the proposed scheme and three baseline schemes according to N ($\lambda = 0.3$, $w = 1$).

Chapter 5. Conclusion

In this thesis, we have designed two resource management schemes for WiFi and UWB systems, with different goals: to improve radio resource efficiency and to enhance time resource efficiency.

First, we have proposed a two-phase radio resource management (RRM) method composed of channel assignment (CA) and user association for channel load balancing (UA-ChLB) in the dense WLAN environment, where two types of APs (i.e., S-APs, C-APs) supporting dual-band of 2.4 GHz and 5 GHz coexist. In the CA phase, while considering channel usages of neighboring S-APs and interference level of C-APs according to the channel bonding, a centralized controller allocates channel and bandwidth of each AP to minimize interference among the APs. In the UA-ChLB phase, the overall network resource efficiency can be maximized by coordinating the UA between STAs and APs having low channel load under consideration of time varying wireless channel and traffic conditions. In this phase, the centralized controller periodically conducts the centralized UA-ChLB with longer period, and each STA can alter its serving AP and/or the serving channel at any time through the distributed UA-ChLB.

Next, we have proposed a time resource management (TRM) method for IEEE 802.15.4z based UWB ranging systems which can provide highly precise spatial awareness and indoor localization services. Since requirements for a ranging interval that may be different according to each application or device type, a Markov decision process based ranging interval decision scheme is designed to enhance the energy efficiency and satisfaction degree of UWB ranging devices (RDEVs).

It has been shown by experimental and simulation results that the proposed RRM method for dense WLAN environment achieves its design goal and outper-

forms existing schemes from view point of throughput and fairness. Furthermore, we have discussed the implementation of the proposed RRM scheme. In addition, it has been shown by simulation results that the proposed TRM for UWB ranging systems outperforms existing schemes for the energy efficiency and satisfaction level of RDEVs.

Bibliography

[1] M. Cheong, H. J. Kwon, J. S. Lee, and S. K. Lee, "Wi-Fi interference measurement in Korea (Part I)," IEEE 802.11-13/0556r1, May 2013.

[2] S. Chieochan, E. Hossain, and J. Diamond, "Channel assignment schemes for infrastructure-based 802.11 WLANs: A survey," *IEEE Commun. Surveys Tutorials*, vol. 12, no. 1, pp. 124–136, Feb. 2010.

[3] Linux wireless, "ACS: Automatic channel selection," [Online]. Available: https://wireless.wiki.kernel.org/en/users/documentation/acs, [Accessed:29-Nov-2020].

[4] B. Bellalta, A. Checco, A. Zocca, and J. Barcelo, "On the interactions between multiple overlapping WLANs using channel bonding," *IEEE Trans. Vehi Tech.*, vol. 65, no. 2, pp. 796–812, Feb. 2016.

[5] P. Kulkarni, Z. Zhong, and F. Cao, "Moving away from the crowd: Channel selection in uncoordinated unplanned dense wireless LANs," in *Proc. ACM SAC'17*, Marakesh, Morocco, Apr. 2017.

[6] T. H. Lim, W. S. Jeon, and D. G. Jeong, "Centralized channel allocation scheme in densely deployed 802.11 wireless LANs," in *Proc. IEEE ICACT'16*, Pyeongchang, Korea, Mar. 2016.

[7] M. Seyedebrahimi, A. Raschella, M. Mackay, and Q. Shi, "SDN-based channel assignment algorithm for interference management in dense Wi-Fi networks," in *Proc. Eur. Conf. Netw. Commun. (EuCNC)*, Athens, Greece, Jun. 2016.

[8] S. Jang and S. Park, "A channel allocation algorithm for reducing the channel sensing/reserving asymmetry in 802.11ac networks," *IEEE Trans. Mobile Comput.*, vol. 14, no. 3, pp. 458–472, Mar. 2015.

[9] M. H. Dwijaksara, W. S. Jeon, and D. G. Jeong, "A centralized channelization scheme for wireless LANs exploiting channel bonding," in *Proc. ACM SAC'18*, Pau, France, Apr. 2018.

[10] D. Gong and Y. Yang, "On-line AP association algorithm for 802.11n WLANs with heterogeneous clients," *IEEE Trans. Comput.*, vol. 63, no. 11, pp. 2772–2786, Nov. 2014.

[11] P. B. Oni and S. D. Blostein, "Decentralized AP selection in large-scale wireless LANs considering multi-AP interference," in *Proc. IEEE ICNC'17*, Santa Clara, USA, Jan. 2017.

[12] H. Kim, W. Lee, M. Bae, and H. Kim, "Wi-Fi seeker: A link and load aware AP selection algorithm," *IEEE Trans. Mobile Comput.*, vol. 16, no. 8, pp. 2366–2378, Aug. 2017.

[13] S. Yang, M. Krishnan, and A. Zakhor, "Access point selection for multi-rate IEEE 802.11 wireless LANs," in *Proc. IEEE Globecom'15*, San Diego, USA, Dec. 2015.

[14] O. B. Karimi, J. Liu, and J. Rexford, "Optimal collaborative access point association in wireless networks," in *Proc. IEEE INFOCOM'14*, Toronto, Canada, Apr. 2014.

[15] A. Raschella, F. Bouhafs, M. Seyedebrahimi, M. Mackay, and Qi. Shi, "Quality of service oriented access point selection framework for large Wi-Fi networks," *IEEE Trans. Netw. Serv. Manage.*, vol. 14, no. 2, pp. 441–454, Jun. 2017.

[16] T. Lei, X. Wen, Z. Lu, and Y. Li, "A semi-matching based load balancing scheme for dense IEEE 802.11 WLANs," *IEEE Access*, vol. 5, pp. 15332–15339, Jul. 2017.

[17] M. H. Dwijaksara, W. S. Jeon, and D. G. Jeong, "A joint user association and load balancing scheme for wireless LANs supporting multicast transmission," in *Proc. ACM SAC'16*, Pisa, Italy, Apr. 2016.

[18] Aruba Networks, "How does band steering and band balancing work in 6.3," [Online]. Available: http://community.arubanetworks.com/t5/Controller-Based-WLANs/How-does-band-steering-and-band-balancing-work-in-6-3/ta-p/184412, [Accessed:29-Nov-2020].

[19] Qualcomm, "Band-Steering for Dual-Band Wi-Fi Access Points," [Online]. Available: https://www.qualcomm.com/documents/band-steering-dual-band-wi-fi-access-points. [Accessed:29-Nov-2020].

[20] D. Okuhara, F. Shiotani, K. Yamamoto, T. Nishio, M. Morikura, R. Kudo, and K. Ishihara, "Attenuators enabled inversely proportional transmission power and carrier sense threshold setting in WLANs," in *Proc. IEEE PIMRC*, Montreal, Washington, USA, Sept. 2014.

[21] D. Okuhara, F. Shiotani, K. Yamamoto, T. Nishio, M. Morikura, R. Kudo, and K. Ishihara, "Inversely proportional transmission power and carrier sense

threshold setting for WLANs: Experimental evaluation of partial settings," in *Proc. IEEE VTC 2016-Fall*, Montreal, Canada, Sept. 2016.

[22] L. Massoulie and J. Roberts, "Bandwidth sharing: Objectives and algorithms," *IEEE/ACM Trans. Netw.*, vol. 10, no. 3, pp. 320–328, June 2002.

[23] V. Angelakis, S. Papadakis, V. A. Siris, and A. Traganitis, "Adjacent channel interference in 802.11a is harmful: Testbed validation of a simple quantification model," *IEEE Commun. Mag.*, vol. 49, no. 3, pp. 160–166, Mar. 2011.

[24] V. Angelakis, A. Traganitis and V. Siris, "Adjacent channel interference in a multi-radio wireless mesh node with 802.11 a/g interfaces," in *Proc. IEEE INFOCOM 2007*, Anchorage, USA, May 2007.

[25] T. Ibaraki, H. Ishii, J. Iwase, T. Hasegawa, and H. Mine, "Algorithms for quadratic fractional programming problems," in *Journal of the Operations Research*, vol. 19, no. 2, pp. 174–191, June 1976.

[26] IBM, IBM ILOG CPLEX, [Online]. Available: http://www-01.ibm.com/software/commerce/optimization/cplex-optimizer, [Accessed:29-Nov-2020].

[27] W. Dinkelbach, "On nonlinear fractional programming," in *Management Science*, vol. 13, no. 7, pp. 492–498, Mar. 1967.

[28] A. M. Voicu, L. Lava, L. Simic, and M. Petrova, "The importance of adjacent channel interference: experimental validation of ns-3 for dense Wi-Fi networks," in *Proc. ACM MSWiM 2017*, Miami, USA, Nov. 2017.

[29] "Wi-Fi adjacent channel interference model for ns-3," [Online]. Available: https://github.com/avoinets/Wi-Fi-ACI-in-ns-3, [Accessed:29-Nov-2020].

[30] L. E. Lima, B. Y. L. Kimura, and V. Rosset, "Experimental environments for Internet of Things: A review," *IEEE Sensors Journal*, vol. 19, no. 9, pp. 3203–3211, May 2019.

[31] M. Mayer and A. J. Baeumner, "A megatrend challenging analytical chemistry: Biosensor and chemosensor concepts ready for the Internet of Things," *Chem. Rev.*, vol. 119, no. 13, pp. 7996–8027, May 2019.

[32] M. A. A. Mamun and M. R. Yuce, "Sensors and systems for wearable environmental monitoring toward IoT-enabled applications: A review," *IEEE Sensors Journal*, vol. 19, no. 18, pp. 7771–7788, Sept. 2019.

[33] 3GPP TS 36.211 version 14.3.0 Release 14, "Evolved universal terrestrial radio access (E-UTRA); physical channels and modulation," Aug. 2017.

[34] W. S. Jeon, S. B. Seo, and D. G. Jeong, "Effective frequency hopping pattern for ToA estimation in NB-IoT random access," *IEEE Trans. Veh. Technol.*, vol. 67, no. 10, pp. 10150–10154, Oct. 2018.

[35] LoRa Alliance Technical Committee, "LoRaWAN^{TM} 1.1 specification," LoRa Alliance Inc., Beaverton, OR, ver. 1.1, Oct. 2017.

[36] LoRa Alliance Technical Committee Regional Parameters Workgroup, "LoRaWAN^{TM} 1.1 regional parameters," LoRa Alliance Inc., San Ramon, CA, Revision B, Jan. 2018.

[37] W. S. Jeon and D. G. Jeong, "Adaptive uplink rate control for confirmed class A transmission in LoRa networks," *IEEE Internet of Things Journal*, Early Access, Apr. 2020.

[38] Bluetooth SIG, "Bluetooth Core Specification Version 4.2," Dec. 2015.

[39] W. S. Jeon, M. H. Dwijaksara, and D. G. Jeong, "Performance analysis of neighbor discovery process in Bluetooth Low Energy networks," *IEEE Trans. Veh. Technol.*, vol. 66, no. 2, pp. 1865–1871, Feb. 2017.

[40] W. S. Jeon and D. G. Jeong, "Enhanced channel access for connection state of Bluetooth Low Energy networks," *IEEE Trans. Veh. Technol.*, vol. 66, no. 9, pp. 8469–8481, Sept. 2017.

[41] IEEE Std 802.15.4z Task Group for WPANs, "Draft Standard for Low-Rate Wireless Networks - Amendment: Enhanced Ultra Wide Band (UWB) Physical layers (PHYs) and Associated Ranging Techniques," Apr. 2019.

[42] IEEE Std 802.15.4a-2007, "Amendment to 802.15.4-2006: Wireless Medium Access Control (MAC) and Physical Layer (PHY) Specifications for Low-Rate Wireless Personal Area Networks (LR-WPANs)," 2007.

[43] IEEE Std 802.15.4f-2012, "Amendment to 802.15.4-2012: Active Radio Frequency Identification (RFID) System Physical Layer (PHY) Specificatons for Low-Rate Wireless Personal Area Networks (LR-WPANs)," 2012.

[44] IEEE Std 802.15-2015, "Standard for Low-Rate Wireless Networks (Revision of IEEE Std 802.15.4-2011)," 2015.

[45] P. Sedlacek, M. Slanina, and P. Masek "An overview of the IEEE 802.15.4z standard and its comparison to the existing UWB standards," in *Proc. IEEE RADIOELEKTRONIKA'19*, Pardubice, Czech Republic, Apr. 2019.

[46] Fira consortium, [online]. Available: https://www.firaconsortium.org/ [Accessed:29-Nov-2020].

[47] D. Neirynck, E. Luk, and M. McLaughlin, "An alternative double-sided two-way ranging method," in *Proc. IEEE WPNC'16*, Bremen, Germany, Oct. 2016.

[48] Google, "Android opensource project for UWB API," [online]. Available: https://android-review.googlesource.com/q/uwb [Accessed:29-Nov-2020].

요약(국문초록)

오늘날 모바일 기기를 통한 멀티미디어 컨텐츠 전송, 초고화질 비디오 스트리밍, 파일 다운로드 등을 효과적으로 지원하기 위해 IEEE 802.11 기반 무선랜 기술들이 널리 이용되고 있다. 또한, 공장/사무실 환경에서의 인적/물적 자원 추적, 위치 기반 스마트홈 어플리케이션 등 다양한 위치 기반 서비스에서 사용될 고정밀 실내 측위를 지원하는 IEEE 802.15.4z 기반 초광대역(UWB: ultra-wideband) ranging 기술이 주목을 받고 있다. 본 논문에서는 WiFi 기기의 처리량 성능 및 UWB 기기의 에너지 효율 등의 요구사항을 만족시키기 위해 해당 기기들을 효과적으로 지원하고 관리하는 무선 자원 관리 방법들을 제안하였다. 먼저, 무선랜 access point (AP)들이 밀집한 환경에서의 전파 자원 관리 방법을 설계하였다. 제안하는 전파 자원 관리 방법은 다음의 두 단계로 구성된다. 첫 번째 단계는 채널 할당 단계로 중앙집중형 제어기의 관리를 받는 중앙형 AP와 개별적으로 동작하는 개별형 AP가 밀집 혼재하는 상황에서 개별형 AP들의 사용 채널 현황과 중앙형 AP들의 채널 본딩 하에서 주채널 사용에 따른 간섭 정도를 고려하여 주변 AP간 간섭을 최소화하도록 중앙형 AP들의 사용 채널과 대역폭을 결정한다. 두 번째 단계는 사용자 연결 조정을 통한 채널 부하 분산 단계로 채널별 부하량을 고려하여 전체 네트워크의 무선 자원 효율을 최대화하도록 중앙집중형 제어기가 비교적 긴 주기로 AP-사용자간 연결을 조정하며, 시시각각 변하는 무선 채널 상황 및 트래픽 상황을 고려하여 사용자 기기도 분산적으로 채널 부하량이 적은 AP로 연결을 조정한다. 다음으로, 고정밀 실내 측위 서비스를 지원하는 IEEE 802.15.4z 기반 UWB ranging 시스템에서 기기들의 에너지 효율 및 서비스 만족도를 향상시키기 위한 시간 자원 관리 방법을 제안하였다. 어플리케이션 용도 또는 기기 종류에 따라 ranging 수행 간격에 대한 요구사

항이 다른 여러 기기들이 속한 ranging 그룹의 ranging 수행 간격을 효과적으로 결정하기 위해 에너지 효율 및 서비스 만족도를 함께 고려하여 최적의 ranging 수행 간격을 결정하는 기법을 마코브 의사 결정 (Markov decision process)에 따라 설계하였다. 제안하는 무선랜 시스템을 위한 전파 자원 관리 기법이 기존의 기법들보다 처리량 및 공정성에 대해 상당히 우수한 성능을 보임을 시뮬레이션과 실제 구현을 통한 실험을 통해 확인하였다. 또한, UWB ranging 시스템을 위한 시간 자원 관리 기법이 에너지 효율과 서비스 만족도에 대해서 기존의 기법들에 비해 우수한 성능을 보임을 시뮬레이션을 통해 확인하였다.